TABLE 1 Associations of serum chemerin levels with clinical symptoms and organ involvement in SSc

Clinical symptoms	Serum chemerin level, ng/ml		*P*-value
	Patients with symptoms	Patients without symptoms	
RP	252.8 (186.3–295.3) ($n=44$)	184.8 (119.1–229.9) ($n=8$)	0.066
Nail fold bleeding	233.4 (178.0–280.0) ($n=30$)	257.7 (176.5–303.6) ($n=20$)	0.99
Pitting scars	252.8 (178.3–307.6) ($n=17$)	233.4 (176.9–285.1) ($n=34$)	0.18
Digital ulcers	264.8 (204.4–319.0) ($n=14$)	232.8 (163.7–285.2) ($n=37$)	0.033
Elevated RVSP	272.5 (194.9–297.2) ($n=9$)	233.9 (172.9–288.1) ($n=43$)	0.19

Data are given as median (25th–75th percentile). Elevated right ventricular systolic pressure (RVSP) was defined as $\geqslant$35 mmHg on echocardiogram.

The association of chemerin with fibrosis has been well studied in synovial fibroblasts since chemerin appears to be involved in the joint inflammation and remodelling of RA, OA and PsA. The concentration of chemerin is elevated in SF of patients with these diseases and chemerin is secreted in cell culture supernatants of synovial fibroblasts [16]. Synovial fibroblasts express ChemR23 and produce Toll-like receptor 4 and CCL2 in response to exogenous chemerin stimulation [17]. Given that Toll-like receptor 4 amplifies TGF-β stimulation in fibroblasts [34, 35] and CCL2 activates fibroblasts directly and indirectly through the recruitment of inflammatory cells [36], chemerin may contribute to the activation of synovial fibroblasts, leading to pathological joint remodelling. In contrast, chemerin expression was decreased in SSc dermal fibroblasts as a result of autocrine TGF-β and Fli1 deficiency in dermal fibroblasts of BLM-treated mice. Taken together with the evidence that chemerin has a pro-fibrotic effect on synovial fibroblasts, chemerin may be suppressed as a result of a negative feedback system in dermal fibroblasts under a pro-fibrotic condition. Alternatively, considering that TGF-β stimulation generally suppresses a set of anti-fibrotic genes in dermal fibroblasts, chemerin may be related to an anti-fibrotic response in the skin. Supporting the latter idea, chemerin expression in dermal fibroblasts is markedly elevated in psoriatic skin lesions [11], which usually develop and regress without accompanying dermal fibrotic response. Further studies are required to address this issue in the future.

The chemerin/ChemR23 axis is a signalling pathway regulating endothelial cell behaviour during angiogenesis. Chemerin promotes the degradation of vascular basement membrane via induction of MMP2 and MMP9 gelatinolytic activity and induces migration, proliferation and capillary-like tube formation to a similar extent to VEGF in microvascular endothelial cells *in vitro* [12, 13]. In SSc lesional skin, chemerin expression was elevated in dermal small blood vessels, suggesting the contribution of the activated chemerin/ChemR23 pathway to the development of SSc vasculopathy, especially digital ulcers and RP as shown in the analysis of patients' sera. Importantly, Fli1 knockdown induced chemerin expression in HDMECs, and $Fli1^{+/-}$ mice expressed this molecule in dermal small blood vessels at higher levels than wild-type mice. Given that Fli1 deficiency is related to the induction of the SSc vascular phenotype, the present findings further support the notion that endothelial Fli1 deficiency alters the angiogenic/angiostatic signalling pathways, including the chemerin/ChemR23 axis, leading to the development of SSc vasculopathy.

Proliferative obliterative vasculopathy is mainly caused by the proliferation of endothelial cells and/or vascular smooth muscle cells in arterioles and small arteries. In this study, the presence of RP and digital ulcers, both of which are associated with proliferative obliterative vasculopathy, was linked to an increase in serum chemerin levels among SSc patients with normal renal function, whereas elevated RVSP did not affect serum chemerin levels. Therefore chemerin may be involved in the development of cutaneous proliferative obliterative vasculopathy in SSc patients. As for renal vascular involvement related to SSc, which is also caused by proliferative obliterative vasculopathy, serum chemerin levels were inversely and significantly correlated with renal dysfunction. This strong correlation suggests the elevation of serum chemerin levels due to a decrease in its clearance, but the contribution of chemerin to proliferative obliterative vasculopathy in the kidney has not yet been ruled out. Additional studies are necessary to clarify this point.

A major limitation of this study is the small number of patients enrolled in the serum study and the lack of studies evaluating the function of chemerin in SSc animal models. Therefore further studies with a larger number of SSc patients and chemerin-deficient or transgenic mice are required to draw a definitive conclusion on the role of chemerin in the pathogenesis of SSc.

In summary, this is the first study demonstrating the potential role of chemerin in SSc. The present study supports the notion that chemerin contributes to the pathological process of various inflammatory and autoimmune diseases through its pleiotropic effects and that Fli1 deficiency is an important factor orchestrating the expression of angiogenesis-related genes in SSc.

Acknowledgements

We thank A. Hatsuta, W. Furuya and T. Kaga for tissue processing and staining and C. Ohwashi, T. Ikegami and N. Watanabe for technical assistance.

Funding: This work was supported by a grant for Research on Intractable Diseases from the Ministry of Health, Labour, and Welfare of Japan.

Disclosure statement: The authors have declared no conflicts of interest.

References

1 Abraham DJ, Krieg T, Distler J, Distler O. Overview of pathogenesis of systemic sclerosis. Rheumatology 2009; 48(Suppl 3):iii3–7.

2 Asano Y. Future treatments in systemic sclerosis. J Dermatol 2010;37:54–70.

3 Masui Y, Asano Y, Shibata S *et al.* Serum adiponectin levels inversely correlate with the activity of progressive skin sclerosis in patients with diffuse cutaneous systemic sclerosis. J Eur Acad Dermatol Venereol 2012;26:354–60.

4 Masui Y, Asano Y, Takahashi T *et al.* Clinical significance of monitoring serum adiponectin levels during intravenous pulse cyclophosphamide therapy in interstitial lung disease associated with systemic sclerosis. Mod Rheumatol 2013;23:323–9.

5 Masui Y, Asano Y, Shibata S *et al.* A possible contribution of visfatin to the resolution of skin sclerosis in patients with diffuse cutaneous systemic sclerosis via a direct anti-fibrotic effect on dermal fibroblasts and Th1 polarization of the immune response. Rheumatology 2013;52:1239–44.

6 Masui Y, Asano Y, Akamata K *et al.* Serum resistin levels: a possible correlation with pulmonary vascular involvement in patients with systemic sclerosis. Rheumatol Int 2014;34: 1165–70.

7 Aozasa N, Asano Y, Akamata K *et al.* Serum apelin levels: clinical association with vascular involvements in patients with systemic sclerosis. J Eur Acad Dermatol Venereol 2013;27:37–42.

8 Toyama T, Asano Y, Takahashi T *et al.* Clinical significance of serum retinol binding protein-4 levels in patients with systemic sclerosis. J Eur Acad Dermatol Venereol 2013; 27:337–44.

9 Ernst MC, Sinal CJ. Chemerin: at the crossroads of inflammation and obesity. Trends Endocrinol Metab 2010; 21:660–7.

10 Bondue B, Wittamer V, Parmentier M. Chemerin and its receptors in leukocyte trafficking, inflammation and metabolism. Cytokine Growth Factor Rev 2011;22:331–8.

11 Albanesi C, Scarponi C, Pallotta S *et al.* Chemerin expression marks early psoriatic skin lesions and correlates with plasmacytoid dendritic cell recruitment. J Exp Med 2009;206:249–58.

12 Bozaoglu K, Curran JE, Stocker CJ *et al.* Chemerin, a novel adipokine in the regulation of angiogenesis. J Clin Endocrinol Metab 2010;95:2476–85.

13 Kaur J, Adya R, Tan BK, Chen J, Randeva HS. Identification of chemerin receptor (ChemR23) in human endothelial cells: chemerin-induced endothelial angiogenesis. Biochem Biophys Res Commun 2010;391: 1762–8.

14 Wang N, Wang QJ, Feng YY, Shang W, Cai M. Overexpression of chemerin was associated with tumor angiogenesis and poor clinical outcome in squamous cell carcinoma of the oral tongue. Clin Oral Investig 2014;18: 997–1004.

15 Banas M, Zabieglo K, Kasetty G *et al.* Chemerin is an antimicrobial agent in human epidermis. PLoS One 2013; 8:e58709.

16 Kaneko K, Miyabe Y, Takayasu A *et al.* Chemerin activates fibroblast-like synoviocytes in patients with rheumatoid arthritis. Arthritis Res Ther 2011;13:R158.

17 Eisinger K, Bauer S, Schäffler A *et al.* Chemerin induces CCL2 and TLR4 in synovial fibroblasts of patients with rheumatoid arthritis and osteoarthritis. Exp Mol Pathol 2012;92:90–6.

18 Asano Y, Ihn H, Yamane K, Kubo M, Tamaki K. Impaired Smad7-Smurf-mediated negative regulation of TGF-β signaling in scleroderma fibroblasts. J Clin Invest 2004; 113:253–64.

19 Ichimura Y, Asano Y, Akamata K *et al.* Fli1 deficiency contributes to the suppression of endothelial CXCL5 expression in systemic sclerosis. Arch Dermatol Res 2014; 306:331–8.

20 Asano Y, Ihn H, Yamane K *et al.* Increased expression of integrin aVb3 contributes to the establishment of autocrine TGF-β signaling in scleroderma fibroblasts. J Immunol 2005;175:7708–18.

21 Asano Y, Ihn H, Yamane K, Jinnin M, Tamaki K. Increased expression of integrin αvβ5 induces the myofibroblastic differentiation of dermal fibroblasts. Am J Pathol 2006; 168:499–510.

22 Asano Y, Czuwara J, Trojanowska M. Transforming growth factor-β regulates DNA binding activity of transcription factor Fli1 by p300/CREB-binding protein-associated factor-dependent acetylation. J Biol Chem 2007; 282:34672–83.

23 Yoshizaki A, Iwata Y, Komura K *et al.* CD19 regulates skin and lung fibrosis via Toll-like receptor signaling in a model of bleomycin-induced scleroderma. Am J Pathol 2008; 172:1650–63.

24 Preliminary criteria for the classification of systemic sclerosis (scleroderma). Subcommittee for scleroderma criteria of the American Rheumatism Association Diagnostic and Therapeutic Criteria Committee. Arthritis Rheum 1980;23:581–90.

25 Asano Y, Ihn H, Yamane K, Kubo M, Tamaki K. Increased expression levels of integrin αvβ5 on scleroderma fibroblasts. Am J Pathol 2004;164:1275–92.

26 Asano Y, Ihn H, Yamane K *et al.* Involvement of αvβ5 integrin-mediated activation of latent transforming growth factor β1 in autocrine transforming growth factor β signaling in systemic sclerosis fibroblasts. Arthritis Rheum 2005;52:2897–905.

27 Wang Y, Fan PS, Kahaleh B. Association between enhanced type I collagen expression and epigenetic repression of the FLI1 gene in scleroderma fibroblasts. Arthritis Rheum 2006;54:2271–9.

28 Asano Y, Stawski L, Hant F *et al.* Endothelial Fli1 deficiency impairs vascular homeostasis: a role in scleroderma vasculopathy. Am J Pathol 2010;176:1983–98.

29 Noda S, Asano Y, Akamata K *et al.* A possible contribution of altered cathepsin B expression to the development of

skin sclerosis and vasculopathy in systemic sclerosis. PLoS One 2012;7:e32272.

30 Noda S, Asano Y, Takahashi T *et al.* Decreased cathepsin V expression due to Fli1 deficiency contributes to the development of dermal fibrosis and proliferative vasculopathy in systemic sclerosis. Rheumatology 2013;52:790–9.

31 Hu W, Feng P. Elevated serum chemerin concentrations are associated with renal dysfunction in type 2 diabetic patients. Diabetes Res Clin Pract 2011;91:159–63.

32 Pfau D, Bachmann A, Lössner U *et al.* Serum levels of the adipokine chemerin in relation to renal function. Diabetes Care 2010;33:171–3.

33 Levey AS, Bosch JP, Lewis JB *et al.* A more accurate method to estimate glomerular filtration rate from serum creatinine: a new prediction equation. Modification of Diet in Renal Disease Study Group. Ann Intern Med 1999;130:461–70.

34 Bhattacharyya S, Kelley K, Melichian DS *et al.* Toll-like receptor 4 signaling augments transforming growth factor-β responses: a novel mechanism for maintaining and amplifying fibrosis in scleroderma. Am J Pathol 2013;182:192–205.

35 Seki E, De Minicis S, Osterreicher CH *et al.* TLR4 enhances TGF-β signaling and hepatic fibrosis. Nat Med 2007;13:1324–32.

36 Yamamoto T, Nishioka K. Role of monocyte chemoattractant protein-1 and its receptor, CCR-2, in the pathogenesis of bleomycin-induced scleroderma. J Invest Dermatol 2003;121:510–6.

DOI: 10.1111/exd.12602
www.wileyonlinelibrary.com/journal/EXD

Original Article

A possible contribution of endothelial CCN1 downregulation due to Fli1 deficiency to the development of digital ulcers in systemic sclerosis

Ryosuke Saigusa, Yoshihide Asano, Takashi Taniguchi, Takashi Yamashita, Takehiro Takahashi, Yohei Ichimura, Tetsuo Toyama, Zenshiro Tamaki, Yayoi Tada, Makoto Sugaya, Takafumi Kadono and Shinichi Sato

Department of Dermatology, University of Tokyo Graduate School of Medicine, Tokyo, Japan
Correspondence: Yoshihide Asano, MD, PhD, Department of Dermatology, University of Tokyo Graduate School of Medicine, 7-3-1 Hongo, Bunkyo-ku, Tokyo 113-8655, Japan, Tel.: +81-3-3815-5411, Fax: +81-3-3814-1503, e-mail: yasano-tky@umin.ac.jp

Abstract: CCN1 is a pleiotropic molecule involved in angiogenesis and postnatal vasculogenesis, both of which are impaired in systemic sclerosis (SSc). To elucidate the potential role of CCN1 in the development of SSc, we investigated CCN1 expression in the lesional skin of SSc patients and SSc animal models and the clinical correlation of serum CCN1 levels. CCN1 expression was markedly decreased in dermal small blood vessels of SSc patients compared with those of healthy controls, while comparable between normal and SSc dermal fibroblasts. Transcription factor Fli1, whose deficiency due to epigenetic suppression is implicated in the pathogenesis of SSc, occupied the CCN1 promoter and gene silencing of Fli1 resulted in the reduction of CCN1 expression in human dermal microvascular endothelial cells. Consistently, CCN1 expression was suppressed uniformly and remarkably in dermal blood vessels of $Fli1^{+/-}$ mice and partially in those of endothelial cell-specific Fli1 knockout mice. Furthermore, serum CCN1 levels were significantly decreased in SSc patients with previous and current history of digital ulcers as compared to those without. Collectively, these results suggest that endothelial CCN1 downregulation at least partially due to Fli1 deficiency may contribute to the development of digital ulcers in SSc patients. This study further supports the idea that epigenetic downregulation of Fli1 is a potential predisposing factor in the pathogenesis of SSc.

Key words: angiogenesis – CCN1 – digital ulcers – systemic sclerosis – vasculogenesis

Accepted for publication 19 November 2014

Introduction

Systemic sclerosis (SSc) is a multisystem connective tissue disease characterized by vascular injury, autoimmunity, and fibrosis of the skin and various internal organs (1,2). Although the detailed pathological process of SSc still remains elusive, aberrant vascular remodelling following autoimmunity-mediated vascular injury has been believed to contribute to the development of vasculopathy characteristic of this disease (3–8). It is generally accepted that aberrant vascular remodelling occurs as a result of impaired angiogenesis and vasculogenesis in SSc (9,10). Serum levels of various angiogenic/angiostatic factors are largely altered and mostly suggest the constitutive pro-angiogenic status especially in the active stage of the disease. For instance, serum levels of vascular endothelial growth factor are elevated in SSc patients, especially in its earliest disease stage (11), and serum levels of angiopoietin 2, which reflect a pro-angiogenic status, positively correlate with disease activity and severity of SSc (12). On the other hand, circulating endothelial progenitor cells (CEPs), which play a role in postnatal vasculogenesis, are decreased and functionally impaired in SSc (13–15), partially accounting for the loss of neovascularization following vascular injury in this disease.

CCN1 is a secreted cysteine-rich heparin-binding protein with diverse functions including the regulatory effect on angiogenesis. CCN1 belongs to CCN gene family together with CCN2 (connective tissue growth factor), CCN3 (nephroblastoma) and CCN4/5/6 (Wnt-inducible secreted protein-1, -2 and -3) (16). The role of CCN1 in embryonic neovascularization has been well studied in CCN1 null mice, which indicates the highly impaired angiogenesis despite normal vasculogenesis (17). Supporting this, a line of evidence has demonstrated that CCN1 promotes angiogenesis through its direct binding to integrin $\alpha V\beta 3$ on endothelial cells and the induction of other angiogenic factors, such as vascular endothelial growth factor-A and -C, from dermal fibroblasts (18–20). In contrast to embryonic vasculogenesis, CCN1 contributes to postnatal vasculogenesis mediated by CEPs. CCN1 binds as a soluble factor to CEPs through integrin $\alpha V\beta 3$ and $\alpha M\beta 2$, which aids in the attachment and transmigration of CEPs into the area of neovascularization (21). Furthermore, CCN1 induces the release of various chemokines, cytokines, growth factors and proteolytic enzymes from CEPs leading to endothelial cell proliferation and angiogenesis (21). Thus, CCN1 is a novel molecule involved in both of angiogenesis and postnatal vasculogenesis.

These backgrounds encouraged us to investigate the potential role of CCN1 in the development of SSc. Therefore, in this study, we investigated the expression levels of CCN1 in SSc lesional skin and the mechanism accounting for the altered expression of CCN1 utilizing *in vitro* cell culture system and *in vivo* animal models. Furthermore, we also examined the clinical correlation of serum CCN1 levels in SSc patients.

Methods

Ethics statement

The study was performed according to the Declaration of Helsinki and approved by the ethical committee of The University of Tokyo Graduate School of Medicine. Written informed consent was obtained from all of the patients and healthy controls.

Immunohistochemistry

Immunohistochemistry with Vectastain ABC kit (Vector Laboratories, Burlingame, CA, USA) was performed on formalin-fixed, paraffin-embedded skin sections using anti-CCN1 antibody (Santa Cruz Biotechnology, Santa Cruz, CA, USA). Skin samples were obtained from forearms of seven SSc patients, and seven healthy controls closely matched for age and gender and from the back skin of wild-type and Fli1 muted mice which are previously described (22,23).

Immunofluorescence

Immunofluorescence was carried out with human and murine skin sections, in which goat anti-platelet and endothelial cell adhesion molecule 1 (PECAM1) antibody (Santa Cruz Biotechnology) and rabbit anti-CCN1 antibody (Santa Cruz Biotechnology) were used as primary antibodies, and FITC-conjugated donkey anti-rabbit IgG antibody (Santa Cruz Biotechnology) and Alexa Fluor donkey 555 anti-goat IgG antibody (Invitrogen, Carlsbad, CA, USA) were used as secondary antibodies. Coverslips were mounted using Vectashield with DAPI (Vector Laboratories), and staining was examined using Bio Zero BZ-8000 (Keyence, Osaka, Japan) at 495 nm (green), 565 nm (red) and 400 nm (blue).

Cell cultures

Human dermal fibroblasts were obtained by skin biopsy from the affected areas (dorsal forearm) of six diffuse cutaneous SSc patients with <2 years of skin thickening and from the corresponding area of six closely matched healthy donors. Fibroblasts were cultured in Dulbecco's modified eagle medium with 10% foetal calf serum, 2 mM L-glutamine and the antibiotic antimycotic solution. These cells were individually maintained as monolayers at 37°C in 95% air, 5% CO_2. Human dermal microvascular endothelial cells (HDMECs) were purchased from Takara Bio Inc. (Shiga, Japan) and cultured on collagen-coated tissue culture plates in EBM-2 medium supplemented with the EGM-2 Bullet Kit (Lonza, Walkersville, MD, USA). Experiments were conducted with dermal fibroblasts in passage 3–6 and with HDMECs in passage 3–5.

RNA isolation and reverse transcript (RT)-real time PCR in cultured cells and skin samples

Gene silencing of Fli1 in HDMECs, the generation of a BLM-induced murine SSc model, RNA isolation from those cells and skin tissue and RT-real time PCR were carried out as described previously (24–26). The sequences of primers were as follows: CCN1-forward 5′-AAGAAACCCGGATTTGTGAG-3′, CCN1-reverse 5′-GCTGCATTTCTTGCCCTTT-3′; Ccn1-forward 5′-TGACCTCCTCGGACTCGAT-3′, Ccn1-reverse 5′-GGTTCGGTGCCAAAGACA-3′; FLI1-forward 5′-GGATGGCAAGGAACTGTGTAA-3′, FLI1-reverse 5′-GGTTGTATAGGCCAGCAG-3′; GAPDH-forward 5′-ACCCACTCCTCCACCTTTGA-3′, GAPDH-reverse 5′-CATACCAGGAAATGAGCTTGACAA-3′; Gapdh-forward 5′-CGTGTTCCTACCCCCAATGT-3′, Gapdh-reverse 5′-TGTCATCATACTTGGCAGGTTTCT-3′.

Chromatin immunoprecipitation assay

The chromatin immunoprecipitation (ChIP) assay was carried out using EpiQuik ChIP kit (Epigentek, Farmingdale, NY, USA), as described previously (26). Putative Fli1 transcription factor binding site in the CCN1 promoter was predicted by Tfsitescan. The primers were as follows: CCN1/F-1082, 5′-ATGATTTCAGGCCACTCCAC-3′; CCN1/R-882, 5′-CTTTAGTTCCAGCCCACTGC-3′.

Patients enrolled in the measurement of serum CCN1 levels

Serum samples, frozen at −80°C until assayed, were obtained from 66 SSc patients [63 women, three men; age, median (25–75 percentile): 59.5 years (48.8–68.0); disease duration, 6.0 years (2.0–19.0)] and 20 healthy individuals [19 women, one man; age 54.5 years (45.3–71.5)]. Patients having been treated with corticosteroids or other immunosuppressants prior to their first visits were excluded. Patients were grouped by the LeRoy's classification system (27): 40 with diffuse cutaneous SSc (dcSSc) and 26 with limited cutaneous SSc (lcSSc). All patients fulfilled the criteria proposed by the American College of Rheumatology (28).

The measurement of serum CCN1 levels

Specific enzyme-linked immunosorbent assay kits were used to measure serum CCN1 levels (R & D Systems, Minneapolis, MN, USA). Briefly, polystyrene cups coated with anti-CCN1 antibodies were incubated with 100 μl of assay diluent and 50 μl of serum at room temperature for 2 h. Then, the cups were washed and incubated at room temperature for 2 h with horseradish peroxidase conjugated anti-CCN1 antibodies. Next, the wells were washed again, added with tetramethylbenzidine and incubated at room temperature for 30 min. Finally, sulphuric acid was added to terminate the reaction and the absorbance at 450 nm was measured. Serum CCN1 levels were calculated using standard curve.

Clinical assessment

The definition of disease onset and disease duration and the details of assessment for organ involvement were previously described.(29) Patients with digital ulcers were defined as patients with previous and current history of digital ulcers.

Statistical analysis

Statistical analysis was carried out with one-way ANOVA followed by Turkey *post hoc* test for multiple comparison, with Mann–Whitney *U*-test to compare the distributions of two unmatched groups, with a paired *t*-test for the comparison of paired data after confirming the normal distribution of the data, with Spearman's rank correlation coefficient to evaluate the correlation with clinical data and with Shapiro–Wilk normality test to confirm a normal distribution. Statistical significance was defined as a P value of <0.05.

Results

CCN1 expression is decreased in dermal blood vessels of SSc patients

We initially investigated the expression levels of CCN1 in normal and SSc skin sections by immunohistochemistry. Representative results are shown in Fig. 1a,b. The results of seven closely matched pairs are summarized in Table 1. In healthy controls, CCN1 expression was detected in epidermal keratinocytes, dermal fibroblasts and dermal small blood vessels and small arteries (Fig. 1a). In SSc patients, CCN1 was expressed in epidermal keratinocytes and dermal fibroblasts at comparable levels to those seen in healthy controls although there was a small variation. The most

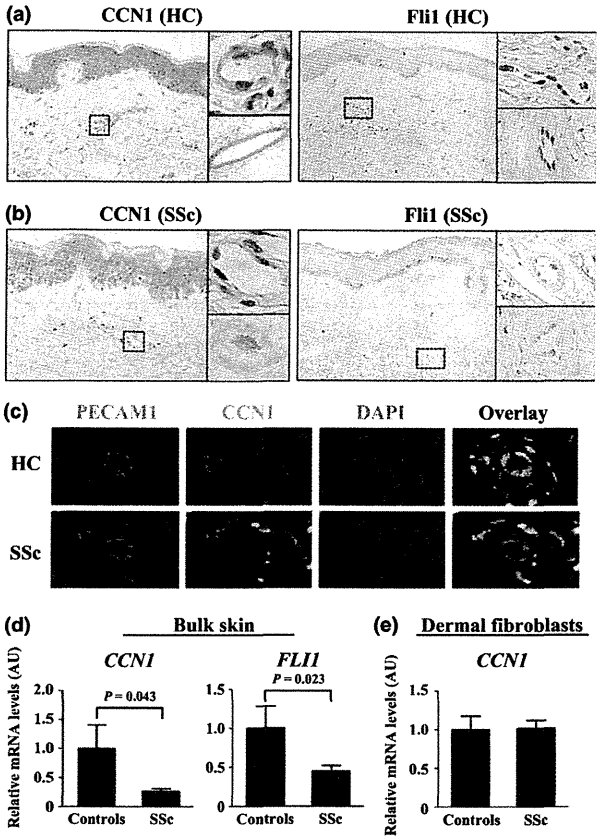

Figure 1. The expression levels of CCN1 in the lesional skin of SSc patients. (a, b) The expression of CCN1 and Fli1 was evaluated by immunohistochemistry in skin sections from healthy controls (HC; a) and SSc patients (b). Representative results are shown (original magnification, ×400). Right upper panels of each picture group depict representative dermal small vessels shown with dotted squares in left panels. Right lower panels of each picture group exhibit dermal small arteries. (c) Immunofluorescence was carried out with DAPI (nuclei; blue) and antibodies against PECAM1 (red) and CCN1 (green) in skin sections from healthy controls (HC) and SSc patients. Representative results of dermal small vessels are shown. (d) mRNA levels of the *CCN1* and *FLI1* genes were determined by RT-real time PCR in normal and SSc skin sections (n = 5 for healthy controls and n = 16 for SSc subjects). (e) mRNA levels of the *CCN1* gene were examined by RT-real time PCR in normal and SSc dermal fibroblasts (n = 6 for both of healthy and control subjects). The relative value compared with controls is expressed as mean ± SEM.

striking difference was observed in dermal small blood vessels and small arteries. In six of seven pairs, CCN1 expression in vascular walls was markedly decreased in SSc skin sections compared with normal skin sections (Fig. 1b). Importantly, co-localization of CCN1 with PECAM1, an established endothelial cell marker, was also confirmed by double immunofluorescence (Fig. 1c). Consistent with this observation, the lesional skin of SSc patients exhibited mRNA levels of the *CCN1* gene significantly lower than the healthy control skin (Fig. 1d), which seems to be at least partially attributable to CCN1 downregulation in SSc dermal small blood vessels. As it is difficult to detect a small difference in the expression levels of target molecules by immunohistochemistry, we also determined the expression levels of CCN1 in cultured normal and SSc dermal fibroblasts by RT-real time PCR. As shown in Fig. 1e, mRNA levels of the *CCN1* gene were comparable between normal and SSc dermal fibroblasts. Collectively, these results indicate that CCN1 expression is decreased in dermal small blood vessels, but not in dermal fibroblasts, of SSc patients.

CCN1 expression is decreased in dermal blood vessels of Fli1$^{+/-}$ mice and endothelial cell-specific Fli1 knockout mice

We next investigated the potential mechanism by which CCN1 expression is suppressed in dermal blood vessels of SSc patients. As Fli1 expression is markedly suppressed at least partially through an epigenetic mechanism in various cell types of SSc skin including dermal microvascular endothelial cells (26,30,31), which was also confirmed in skin samples used in this study (Fig. 1a,b,d), and endothelial Fli1 deficiency reproduces the histopathological and functional abnormalities characteristic of SSc vasculopathy in mice (22), we hypothesized that endothelial Fli1 deficiency inhibits the expression of CCN1 in dermal blood vessels of SSc patients. To address this issue, we examined the effect of Fli1 gene silencing on mRNA levels of the *CCN1* gene in HDMECs. As shown in Fig. 2a, gene silencing of Fli1 resulted in a significant decrease in mRNA levels of the *CCN1* gene in HDMECs (0.68 ± 0.14 fold increase, P = 0.0021). Furthermore, ChIP analysis revealed the binding of Fli1 to the CCN1 promoter in HDMECs (Fig. 2b). These results indicate that Fli1 directly targets the *CCN1* promoter and is required for homeostatic CCN1 expression in endothelial cells. To further confirm whether endothelial Fli1 deficiency results in the downregulation of CCN1 in dermal blood vessels *in vivo*,

Table 1. CCN1 levels in skin sections from SSc patients and healthy controls

Samples	Age/sex	Duration (years)	dcSSc/lcSSc	Keratinocytes	Fibroblasts	Blood vessels
NS1	65 F			++	++	+++
SSc1	60 F	0.1	dcSSc	+++	+	+
NS2	42 F			+++	++	+++
SSc2	48 F	0.7	dcSSc	+++	+	++
NS3	65 F			+++	+	+++
SSc3	68 F	2	dcSSc	++	+	+
NS4	41 F			+++	+	++
SSc4	43 F	2.5	dcSSc	++	+	+
NS5	71 F			+++	+	++
SSc5	70 F	5	dcSSc	+++	+	++
NS6	31 F			+++	+	+++
SSc6	32 F	8	dcSSc	++	+	++
NS7	37 F			+++	+	+++
SSc7	38 F	15	lcSSc	+++	+	+

Disease duration means the interval between the onset defined as the first clinical event of SSc other than Raynaud's phenomenon and the time the blood samples were drawn. NS, normal skin; SSc, systemic sclerosis; dcSSc, diffuse cutaneous systemic sclerosis; lcSSc, limited cutaneous systemic sclerosis. We used the following grading system: +, slight staining; ++, moderate staining; +++, strong staining.

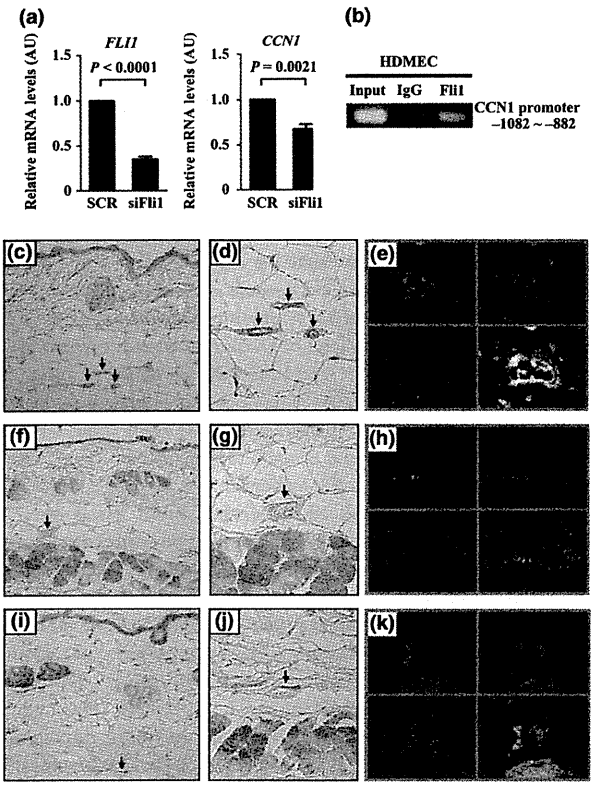

Figure 2. The impact of endothelial Fli1 deficiency on the expression levels of CCN1 *in vivo* and *in vitro*. (a) mRNA levels of the *FLI1* and *CCN1* genes in HDMECs transfected with Fli1 siRNA or non-silencing scrambled RNA (SCR) were measured by RT-real time PCR and normalized to mRNA levels of the *GAPDH* gene. The relative values compared with the controls are expressed as mean ± SEM of six independent experiments. Statistical analysis was carried out with a two-tailed paired *t*-test after confirming the normal distribution of the data. (b) Chromatin was isolated from HDMECs and immunoprecipitation was conducted with rabbit anti-Fli1 antibody or rabbit IgG. PCR amplification was carried out using CCN1 promoter-specific primers. One representative of three independent experiments is shown. (c–k) CCN1 expression in small blood vessels was determined by immunohistochemistry (c, d, f, g, i, j) and immunofluorescence (e, h, k) in the skin sections of 3-month-old wild-type mice (c–e), $Fli1^{+/-}$ mice (f–h) and Fli1 ECKO mice (i–k). Epidermis, dermis and subcutaneous fat tissue are shown in c, f and i (original magnification ×200). Small blood vessels of c, f and i are shown in d, g and j with a higher magnification, respectively. Corresponding vessels are shown with arrows. Immunofluorescence was carried out with DAPI (nuclei; blue) and antibodies against PECAM1 (red) and CCN1 (green). Representative results of small vessels are shown. Representative results of five mice for each strain are shown. Similar staining levels were seen in all the other mice of each strain.

we carried out immunohistochemistry with the skin sections from Fli1 mutated mice. Notably, CCN1 expression was uniformly and totally undetectable in dermal blood vessels of $Fli1^{+/-}$ mice and only partially detectable in those of endothelial cell-specific Fli1 knockout (Fli1 ECKO) mice, while abundantly seen in those of wild-type mice (Fig. 2c,d,f,g,i,j). As previously reported (22), Fli1 mRNA levels are decreased up to 20–50% of baseline in dermal microvascular endothelial cells isolated from Fli1 ECKO mice, suggesting that most of endothelial cells of Fli1 ECKO mice express Fli1 at lower levels than endothelial cells of $Fli1^{+/-}$ mice. Given the variable efficiency of the Cre enzyme in individual endothelial cells (22), in Fli1 ECKO mice Fli1 expression is not affected in some endothelial cells, which theoretically produce CCN1 to a similar extent to wild-type endothelial cells, as shown in Fig. 2i,j.

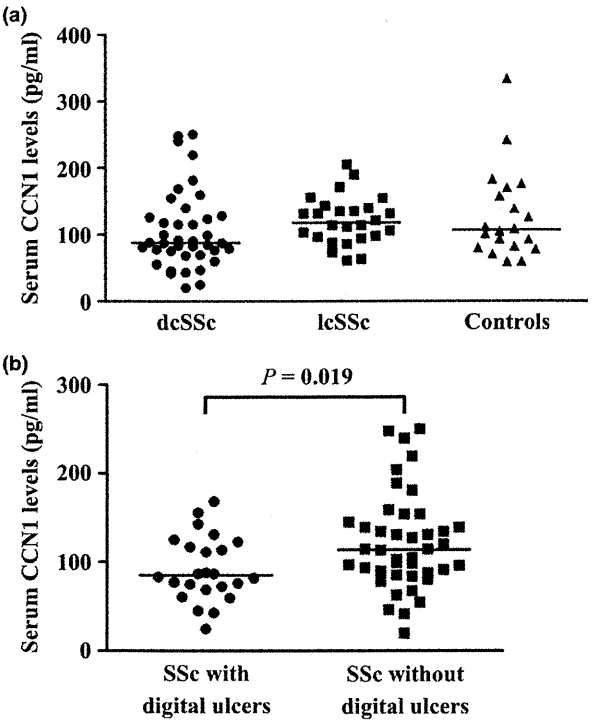

Figure 3. Clinical correlation of serum CCN1 levels in SSc patients. Serum CCN1 levels were measured by a specific ELISA. The levels were compared among dcSSc (n = 40), lcSSc (n = 26), and control subjects (n = 20) (a) and between SSc patients with digital ulcers (n = 24) and those without (n = 42) (b). Horizontal bars represent median of each group.

We also confirmed the colocalization of CCN1 with PECAM1 by double immunofluorescence in murine blood vessels (Fig. 2e,h,k). These results indicate that endothelial Fli1 deficiency induces CCN1 downregulation in dermal blood vessels *in vivo*, suggesting that endothelial Fli1 deficiency contributes to CCN1 suppression in SSc dermal blood vessels.

The decrease in serum CCN1 levels correlates with vascular involvement in SSc patients

We next evaluated the clinical correlation of serum CCN1 levels in SSc patients. As shown in Fig. 3a, serum CCN1 levels were comparable among dcSSc, lcSSc and healthy controls [median (25–75 percentiles); 87.2 pg/ml (70.4–127.0), 117.1 pg/ml (95.4–140.2) and 106.0 pg/ml (80.1–166.3), respectively; P = 0.29, one-way ANOVA]. We also examined the correlation of serum CCN1 levels with dermal and pulmonary fibrotic markers, including modified Rodnan total skin thickness score, the percentage of predicted vital capacity and the percentage of predicted diffusion lung capacity for carbon monoxide, but failed to detect any significant correlation (data not shown).

As CCN1 is downregulated in dermal small blood vessels of SSc as described above, we further looked at the correlation of serum CCN1 levels with clinical symptoms relevant to SSc vasculopathy, such as Raynaud's phenomenon, nailfold bleeding, telangiectasia, digital ulcers, pulmonary arterial hypertension and scleroderma renal crisis. To this end, serum CCN1 levels were compared between SSc patients with each symptom and those without. The

presence of cutaneous vascular symptoms, including Raynaud's phenomenon, nailfold bleeding and telangiectasia, did not affect serum CCN1 levels [patients with symptoms versus those without; 103.1 (80.7–134.6) pg/ml vs 91.3 (41.6–139.3) pg/ml ($P = 0.35$) for Raynaud's phenomenon, 101.3 (81.9–134.6) pg/ml vs 113.6 (74.8–155.6) pg/ml ($P = 0.95$) for nailfold bleeding, 87.8 (73.6–132.9) pg/ml vs 106.6 (78.9–154.1) pg/ml ($P = 0.34$) for telangiectasia]. Regarding organ involvement associated with proliferative obliterative vasculopathy, SSc patients with digital ulcers had serum CCN1 levels significantly lower than those without [84.9 (69.8–121.5) pg/ml vs 114.2 (87.2–147.4) pg/ml ($P = 0.019$), Fig. 3b], while the presence of elevated right ventricular systolic pressure or scleroderma renal crisis did not alter serum CCN1 levels in SSc patients [113.6 (72.5–134.6) pg/ml vs 99.5 (78.4–142.8) pg/ml ($P = 0.73$) for elevated right ventricular systolic pressure, 98.9 (39.6–144.2) pg/ml vs 101.3 (78.1–135.8) pg/ml ($P = 0.62$) for scleroderma renal crisis]. Importantly, serum CCN1 levels were decreased in SSc patients with digital ulcers than in healthy controls ($P = 0.045$), while comparable between SSc patients without digital ulcers and healthy controls ($P = 0.75$). These results suggest that the decreased expression of CCN1 in dermal small blood vessels is linked to the development of digital ulcers in SSc patients.

Discussion

It is generally accepted that the impairment of angiogenesis in response to vascular injury is a potential mechanism leading to progressive vascular and fibrotic complications in SSc (9,10,13,15,32,33). Therefore, this study was undertaken to investigate the potential role of CCN1 in the developmental process of SSc. In accordance with the critical role of CCN1 in regulating the behaviour of endothelial cells during vascular remodelling (17–21), the altered expression of CCN1 was prominent in dermal small blood vessels and small arteries of SSc patients. As shown by the analysis of serum CCN1 levels, SSc patients with digital ulcers had serum CCN1 levels significantly lower than the other patients. As soluble molecules released from endothelial cells are much more easily accessible to blood stream than those secreted from keratinocytes and fibroblasts, the decrease in serum CCN1 levels may be mainly attributable to the downregulation of CCN1 in vascular walls. Therefore, the close association of low serum CCN1 levels with current and previous history of digital ulcers suggests a possible association of endothelial CCN1 deficiency with the development of digital ulcers in SSc patients. Given that digital ulcers associated with SSc are largely attributable to aberrant vascular remodelling (9,10), CCN1 may be a member of soluble factors involved in the pathological process underlying SSc vasculopathy.

The expression profile of pericyte markers in dermal small blood vessels represents the constitutive pro-angiogenic status of SSc lesional skin, namely, the increased expression of Rgs5, a marker of pericytes with pro-angiogenic phenotype and the decreased expression of α-smooth muscle actin, a marker of pericytes with angiostatic phenotype (22,34). However, various clinical data have revealed the complicated vascular events in SSc, which is characterized by altered serum levels of various angiogenic/angiostatic molecules. Most of the data imply the constitutive activation of angiogenesis, while the others suggest the defective angiogenesis (9,10). Although the detailed molecular mechanisms accounting for the complicated vascular events in SSc still remain unknown, our previous studies have disclosed that Fli1 ECKO mice recapitulate the morphologically and functionally abnormal blood vessels characteristic of SSc vasculopathy, such as stenosis of arterioles, dilation of capillaries and increased vascular permeability (22). Furthermore, endothelial Fli1 deficiency contributes to the altered expression of angiogenesis-related molecules, such as VE-cadherin, PECAM1, platelet-derived growth factor-B, matrix metalloproteinase 9, cathepsin V, cathepsin B and CXCL5, in SSc dermal microvascular endothelial cells (22,26,35,36). These results suggest the critical contribution of endothelial Fli1 deficiency to the development of SSc vasculopathy. Based on this idea, we examined the effect of Fli1 deficiency on the expression levels of the *CCN1* gene *in vivo* and *in vitro*. Notably, gene silencing of Fli1 significantly suppressed mRNA levels of the *CCN1* gene and Fli1 occupied the CCN1 promoter. Furthermore, CCN1 expression was markedly reduced in dermal small blood vessels of Fli1 mutated mice. These results indicate that CCN1 is a member of angiogenesis-related molecules directly regulated by Fli1 and closely involved in the pathological angiogenesis of SSc.

The impairment of CEPs has been well studied in the research field of SSc by focusing on the number and the property of CEPs (13–15,32,33). On the other hand, the recruitment of CEPs to injured vascular areas is another important step in the regulation of postnatal vasculogenesis, in which endothelial cell-derived CCN1 is involved. Dual roles of CCN1 in angiogenesis and postnatal vasculogenesis suggest that this molecule coordinately regulates the complex interplay between the two processes during the physiological vascular remodelling. Therefore, the downregulation of endothelial CCN1 expression may be involved in the defective vasculogenesis of SSc. As far as we know, the mechanism regulating CEP recruitment to injured vessels has not been well examined in SSc. Further studies on CCN1 may provide us a new clue to understand the mechanism underlying defective vasculogenesis of SSc.

In summary, this is the first study evaluating the role of CCN1 in the pathological process of SSc. A series of clinical and laboratory data suggest that endothelial CCN1 downregulation at least partially due to Fli1 deficiency may contribute to the defective angiogenesis characteristically seen in SSc, leading to the development of digital ulcers. This study further supports the idea that epigenetic downregulation of Fli1 is a potential predisposing factor in the pathogenesis of SSc (22,31,37,38).

Acknowledgements

We thank A. Hatsuta, W. Furuya and T. Kaga for tissue processing and staining, and C. Ohwashi, T. Ikegami and N. Watanabe for technical assistance. This work was supported by a grant for Research on Intractable Diseases from the Ministry of Health, Labour and Welfare of Japan.

Author contributions

RS and YA performed study conception and design. RS, T Taniguchi, TY, T Takahashi, YI, T Toyama and ZT performed acquisition of data. RS, YA, YT, MS, TK and SS were responsible for analysis and interpretation of data. RS, YA, YT, MS, TK and SS performed drafting and/or critical revision of the manuscript. All authors have read and approved the final manuscript.

Conflict of interests

The authors have declared no conflicting interests.

References

1 Asano Y. J Dermatol 2010: **37**: 54–70.
2 Abraham D J, Krieg T, Distler J *et al.* Rheumatology (Oxford) 2009: **48** (Suppl 3): iii3–iii7.
3 Giacomelli R, Matucci-Cerinic M, Cipriani P *et al.* Arthritis Rheum 1998: **41**: 327–334.
4 Kahaleh M B, Fan P S, Otsuka T. Clin Immunol 1999: **91**: 188–195.
5 Hill M B, Phipps J L, Cartwright R J *et al.* Clin Exp Immunol 1996: **106**: 491–497.
6 Rosenbaum J, Pottinger B E, Woo P *et al.* Clin Exp Immunol 1988: **72**: 450–456.
7 Salojin K V, Le Tonquèze M, Saraux A *et al.* Am J Med 1997: **102**: 178–185.
8 Sgonc R, Gruschwitz M S, Boeck G *et al.* Arthritis Rheum 2000: **43**: 2550–2562.
9 Distler J H, Gay S, Distler O. Rheumatology (Oxford) 2006: **45** (Suppl 3): iii26–iii27.
10 Rabquer B J, Koch A E. Curr Rheumatol Rep 2012: **14**: 56–63.
11 Distler O, Del Rosso A, Giacomelli R *et al.* Arthritis Res 2002: **4**: R11.
12 Michalska-Jakubus M, Kowal-Bielecka O, Chodorowska G *et al.* Rheumatology (Oxford) 2011: **50**: 746–755.
13 Kuwana M, Okazaki Y, Yasuoka H *et al.* Lancet 2004: **364**: 603–610.
14 Kuwana M, Okazaki Y. Ann Rheum Dis 2012: **71**: 617–620.
15 Kuwana M, Okazaki Y. Arthritis Rheum 2014: **66**: 1300–1305.
16 Lau L F. Cell Mol Life Sci 2011: **68**: 3149–3163.
17 Mo F E, Muntean A G, Chen C C *et al.* Mol Cell Biol 2002: **22**: 8709–8720.
18 Chen N, Leu S J, Todorovic V *et al.* J Biol Chem 2004: **279**: 44166–44176.
19 Chen C C, Mo F E, Lau L F. J Biol Chem 2001: **276**: 47329–47337.
20 Leu S J, Lam S C, Lau L F. J Biol Chem 2002: **277**: 46248–46255.
21 Grote K, Salguero G, Ballmaier M *et al.* Blood 2007: **110**: 877–885.
22 Asano Y, Stawski L, Hant F *et al.* Am J Pathol 2010: **176**: 1983–1998.
23 Spyropoulos D D, Pharr P N, Lavenburg K R *et al.* Mol Cell Biol 2000: **20**: 5643–5652.
24 Asano Y, Czuwara J, Trojanowska M. J Biol Chem 2007: **282**: 34672–34683.
25 Yoshizaki A, Iwata Y, Komura K *et al.* Am J Pathol 2008: **172**: 1650–1663.
26 Ichimura Y, Asano Y, Akamata K *et al.* Arch Dermatol Res 2014: **306**: 331–338.
27 LeRoy E, Black C, Fleischmajer R *et al.* J Rheumatol 1988: **15**: 202–205.
28 Subcommittee For Scleroderma Criteria of the American Rheumatism Association Diagnostic and Therapeutic Criteria Committee. Arthritis Rheum 1980: **23**: 581–590.
29 Noda S, Asano Y, Aozasa N *et al.* Arch Dermatol Res 2013: **305**: 325–331.
30 Wang Y, Fan P S, Kahaleh B. Arthritis Rheum 2006: **54**: 2271–2279.
31 Kubo M, Czuwara-Ladykowska J, Moussa O *et al.* Am J Pathol 2003: **163**: 571–581.
32 Yamaguchi Y, Okazaki Y, Seta N *et al.* Arthritis Res Ther 2010: **12**: R205.
33 Yamaguchi Y, Kuwana M. Histol Histopathol 2013: **28**: 175–183.
34 Fleming J N, Nash R A, McLeod D O *et al.* PLoS One 2008: **3**: e1452.
35 Noda S, Asano Y, Takahashi T *et al.* Rheumatology (Oxford) 2013: **52**: 790–799.
36 Noda S, Asano Y, Akamata K *et al.* PLoS One 2012: **7**: e32272.
37 Asano Y, Markiewicz M, Kubo M *et al.* Mol Cell Biol 2009: **29**: 425–434.
38 Asano Y, Bujor A M, Trojanowska M. J Dermatol Sci 2010: **59**: 153–162.

ARTHRITIS & RHEUMATOLOGY
Vol. 67, No. 2, February 2015, pp 517–526
DOI 10.1002/art.38948

Fibrosis, Vascular Activation, and Immune Abnormalities Resembling Systemic Sclerosis in Bleomycin-Treated Fli-1–Haploinsufficient Mice

Takashi Taniguchi,[1] Yoshihide Asano,[1] Kaname Akamata,[1] Shinji Noda,[1] Takehiro Takahashi,[1] Yohei Ichimura,[1] Tetsuo Toyama,[1] Maria Trojanowska,[2] and Shinichi Sato[1]

Objective. **Fli-1, a potential predisposing factor for systemic sclerosis (SSc), is constitutively down-regulated in the lesional skin of patients with SSc by an epigenetic mechanism. To investigate the impact of Fli-1 deficiency on the induction of an SSc phenotype in various cell types, we generated bleomycin-induced skin fibrosis in Fli-1$^{+/-}$ mice and investigated the molecular mechanisms underlying its phenotypic alterations.**

Methods. **Messenger RNA (mRNA) levels and protein expression of target molecules were examined by quantitative reverse transcription–polymerase chain reaction and immunostaining. Transforming growth factor β (TGFβ) bioassay was used to evaluate the activation of latent TGFβ. The binding of Fli-1 to the target gene promoters was assessed with chromatin immunoprecipitation.**

Results. **Bleomycin induced more severe dermal fibrosis in Fli-1$^{+/-}$ mice than in wild-type mice. Fli-1 haploinsufficiency activated dermal fibroblasts via the up-regulation of αvβ3 and αvβ5 integrins and activation of latent TGFβ. Dermal fibrosis in Fli-1$^{+/-}$ mice was also attributable to endothelial-to-mesenchymal transition, which is directly induced by Fli-1 deficiency and amplified by bleomycin. Th2/Th17-skewed inflammation and increased infiltration of mast cells and macrophages were seen, partly due to the altered expression of cell adhesion molecules in endothelial cells as well as the induction of the skin chemokines. Fli-1$^{+/-}$ mouse macrophages preferentially differentiated into an M2 phenotype upon stimulation with interleukin-4 (IL-4) or IL-13.**

Conclusion. **Our findings provide strong evidence for the fundamental role of Fli-1 deficiency in inducing SSc-like phenotypic alterations in dermal fibroblasts, endothelial cells, and macrophages in a manner consistent with human disease.**

Systemic sclerosis (SSc) is a multisystem connective tissue disease characterized by immune abnormalities, vasculopathy, and fibrosis of the skin and certain internal organs (1). It is generally accepted that SSc is caused by the complex interplay between hereditary and environmental factors, leading to the accumulation of predisposing factors and the subsequent activation of endothelial cells, immune cells, and fibroblasts (2). Various combinations of predisposing factors may explain disease heterogeneity and a variety of organ involvement in SSc.

The transcription factor Fli-1, a member of the Ets transcription factor family, is epigenetically suppressed in SSc skin and SSc dermal fibroblasts and may represent such a predisposing factor for SSc (3). Fli-1 expression is decreased in nonlesional SSc skin in various cell types, including dermal fibroblasts, endothelial cells, and perivascular inflammatory cells, suggesting that down-regulation of Fli-1 is an early event preceding the development of fibrosis (4). The factors that might be involved in the down-regulation of Fli-1 include trans-

Supported by the Ministry of Health, Labor, and Welfare of Japan (Research on Intractable Diseases grant), the Japan Intractable Diseases Research Foundation, a Rohto Dermatology Prize, the Japanese Society for Investigative Dermatology (JSID Fellowship Shiseido Award), the Mochida Memorial Foundation for Medical and Pharmaceutical Research, and the Japan Foundation for Applied Enzymology. Dr. Trojanowska's work was supported by NIH grant AR042334.

[1]Takashi Taniguchi, MD, Yoshihide Asano, MD, PhD, Kaname Akamata, MD, PhD, Shinji Noda, MD, PhD, Takehiro Takahashi, MD, Yohei Ichimura, MD, Tetsuo Toyama, MD, Shinichi Sato, MD, PhD: University of Tokyo Graduate School of Medicine, Tokyo, Japan; [2]Maria Trojanowska, PhD: Boston University School of Medicine, Boston, Massachusetts.

Address correspondence to Yoshihide Asano, MD, PhD, Department of Dermatology, University of Tokyo Graduate School of Medicine, 7-3-1 Hongo, Bunkyo-ku, Tokyo 113-8655, Japan. E-mail: yasano-tky@umin.ac.jp.

Submitted for publication February 21, 2014; accepted in revised form November 4, 2014.

forming growth factor β (TGFβ) (4) and interferon-α (5) in addition to epigenetic mechanisms (3).

Fli-1 deficiency induces the SSc phenotype in dermal fibroblasts and dermal microvascular endothelial cells at the molecular level (4–6). In dermal fibroblasts, Fli-1 functions as a potent repressor of the *COL1A1* and *COL1A2* genes (4,6–9), and its deficiency modulates the expression of other fibrosis-related genes, resulting in myofibroblastic differentiation (10–15). In endothelial cells, Fli-1 deficiency suppresses the expression of genes regulating endothelial cell–endothelial cell and endothelial cell–pericyte interactions and up-regulates matrix metalloproteinase 9, thus promoting the remodeling of vascular basement membrane (16). Notably, endothelial cell–specific Fli-1–knockout mice reproduce the histologic and functional abnormalities characteristic of SSc vasculopathy (16). However, endothelial cell–specific Fli-1–knockout or Fli-$1^{+/-}$ mice do not spontaneously develop apparent clinical symptoms of SSc.

Since the complexity of SSc cannot be entirely explained by genetic predisposition, epigenetic components such as Fli-1 deficiency potentially play a critical role in the development of this disease. The previous data regarding Fli-1–deficient mice support this idea and further suggest that some additional factors may synergize with Fli-1 deficiency to promote the development of clinically definite SSc. To assess this hypothesis, we generated a bleomycin-induced murine model of SSc using Fli-$1^{+/-}$ mice and investigated the role of Fli-1 deficiency in the induction of the SSc phenotype by focusing on the key cell types involved in the pathogenesis of SSc.

MATERIALS AND METHODS

Mice. Eight-week-old female C57BL/6 mice were used. Mice were bred from Fli-$1^{+/+}$ × Fli-$1^{+/-}$ parents. The derivation of Fli-$1^{+/-}$ mice has been described previously (17). All studies and procedures were approved by the Committee on Animal Experimentation of the University of Tokyo Graduate School of Medicine.

Bleomycin-induced murine model of SSc. Bleomycin (200 μg) dissolved in phosphate buffered saline (PBS) or control PBS alone was injected subcutaneously into a single location on the backs of the mice daily for 4 weeks (18).

Histologic assessment. On the day after the final injection, skin sections were obtained from the mice postmortem. Sections (6-μm thick) were stained with hematoxylin and eosin (H&E), Masson's trichrome, and toluidine blue. Dermal thickness was examined as previously described (19). Immunohistochemistry was performed using antibodies directed against α-smooth muscle actin (mouse clone 1A4; Sigma-Aldrich), connective tissue growth factor (CTGF/CCN2) (sc-14939; Santa Cruz Biotechnology), β3 integrin (sc-6627; Santa Cruz Biotechnology), β5 integrin (sc-5401; Santa Cruz Biotechnology), CD4 (rat clone 2H9; Relia Tech), CD8 (mouse clone 53-6.7; BD PharMingen), F4/80 (rat clone A3-1; AbD Serotec), and arginase 1 (sc-18531; Santa Cruz Biotechnology). For immunofluorescence, goat anti–VE-cadherin antibody (sc-6458; Santa Cruz Biotechnology), rabbit anti–fibroblast-specific protein 1 (anti–FSP-1) antibody (ab41532; Abcam), goat anti–β3 integrin antibody (sc-6627; Santa Cruz Biotechnology), and goat anti–β5 integrin antibody (sc-5401; Santa Cruz Biotechnology) were used as primary antibodies and fluorescein isothiocyanate–conjugated donkey anti-rabbit IgG antibody (sc-2090; Santa Cruz Biotechnology) and Alexa Fluor 555–conjugated donkey anti-goat IgG antibody (A21432; Invitrogen) were used as secondary antibodies. Coverslips were mounted by using Vectashield with DAPI (Vector), and staining was examined by using Biozero BZ-8000 (Keyence) at 495 nm (green), 565 nm (red), and 400 nm (blue). Ten random grids were evaluated under high magnification by 2 independent researchers (TT and YA) in a blinded manner. All experiments included at least 4 mice per study group.

Hydroxyproline measurement. Using QuickZyme Total Collagen Assay according to the recommendations of the manufacturer (QuickZyme Biosciences), 6-mm punch biopsy skin samples were hydrolyzed with 6*N* HCl, and collagen content was quantified. A standard hydroxyproline solution of 0–6 mg/ml was used to generate a standard curve.

Cell culture. Human dermal fibroblasts, human dermal microvascular endothelial cells (HDMECs), and peritoneal macrophages were prepared and maintained as previously described (8,16,20,21). In some experiments, dermal fibroblasts were treated with 2 ng/ml of TGFβ1 (R&D Systems) and/or 20 μg/ml of RGD or RGE peptides (Takara Bio) for 24 hours, and peritoneal macrophages were stimulated with 20 ng/ml of mouse interleukin-4 (IL-4) or IL-13 (R&D Systems) for 24 hours.

Small interfering RNA (siRNA). Cells were transfected with 10 n*M* Fli-1 siRNA or scrambled nonsilencing RNA (Santa Cruz Biotechnology) for 48 hours using HiPerFect transfection reagent (Qiagen) shortly after seeding. Thereafter, cells were serum starved for 24 hours and subsequently harvested.

RNA isolation and quantitative reverse transcription–polymerase chain reaction (PCR). Total RNA was isolated from the lower back skin of mice and distal one-third of the forearm of SSc patients and healthy controls with RNeasy spin columns (Qiagen). One microgram of RNA was reverse transcribed using iScript cDNA Synthesis kits (Bio-Rad). Real-time quantitative PCR was carried out using SYBR Green PCR Master Mix (Life Technologies) on an ABI Prism 7000 system (Life Technologies) in triplicate. The messenger RNA (mRNA) levels were normalized to those of the GAPDH gene. The relative change in the levels of genes of interest was determined by the $2^{-\Delta\Delta C_t}$ method. Dissociation analysis for each primer pair and reaction was performed to verify specific amplification. The primer sequences used are available online at http://www.h.u-tokyo.ac.jp/der/pg237.html.

TGFβ bioassay. To determine TGFβ activation, transformed mink lung reporter cells (TMLCs) were cocultured with either scrambled nonsilencing RNA–transfected fibroblasts or Fli-1 siRNA–transfected fibroblasts as described previously (22). TMLCs and test cells were mixed at a ratio of 1:1 and suspended at 1 × 10^6 cells/ml in Dulbecco's modified Eagle's medium containing 1% fetal bovine serum. These cells

were plated at 200 μl/well in 12-well plates and cultured for 24 hours. Cell lysates were prepared using Reporter Lysis buffer (Promega), and luciferase activity was determined using a Promega luciferase assay system. In experiments without cell–cell contact, similar cocultures were performed in 24-well plates with inserts designed for attachment-dependent cell culture (Millicell-PCF 3-μm filter; Millipore), but 1.5 $\times$ 10^5 TMLCs and test cells were added to the lower and upper chambers, respectively. In some experiments, fibroblasts were treated with 2 ng/ml of TGFβ1 before coculture with TMLCs, and cocultures were conducted in the presence of 20 μg/ml of RGD or RGE peptides.

Chromatin immunoprecipitation (ChIP) assay. ChIP assay was performed using an EpiQuik ChIP kit (Epigentek). After reversal of crosslinking, the immunoprecipitated chromatin was amplified by PCR of specific regions of target genes. The amplified DNA products were resolved by agarose gel electrophoresis. The putative Fli-1 binding site was predicted by Tfsitescan. Primer sequences are available online at http://www.h.u-tokyo.ac.jp/der/pg237.html.

Extraction of collagen from skin by the acetic acid method. Acetic acid extraction of collagen was performed as previously described (23,24). Skin punches (8 mm) were taken from the back of each mouse. Skin sections were then minced and incubated in 10 volumes of PBS overnight at 4°C with stirring. Tissue was harvested by centrifugation at 12,000*g* for 15 minutes and suspended in 10 volumes of cold 0.5*M* acetic acid with or without the addition of pepsin (1:10 ratio of pepsin to tissue wet weight). Extraction was performed overnight at 4°C with stirring, and the supernatant was dialyzed against 0.1*M* acetic acid. Next, the dialysates with pepsin added were treated with pepstatin A (Sigma-Aldrich), followed by lyophilization. Lyophilized proteins were resuspended in cold 0.1*M* acetic acid and were tumbled for ~20 hours. Equal aliquots from each sample were neutralized with 1*M* Tris base, boiled in sample buffer with the addition of 2-mercaptoethanol, resolved by 6% sodium dodecyl sulfate–polyacrylamide gel electrophoresis, and stained with Coomassie blue. Collagen levels were quantified using ImageJ software (National Institutes of Health).

Statistical analysis. Statistical analysis was carried out using GraphPad Prism. One-way analysis of variance with Bonferroni post hoc test was used for multiple-group comparisons, and unpaired 2-tailed *t*-test was used for 2-group comparisons. For comparing 2 group values that did not follow Gaussian distribution, the 2-tailed Mann-Whitney U test was used. Within-group distributions are expressed as the mean ± SEM. *P* values less than 0.05 were considered significant.

RESULTS

Greater dermal thickness in bleomycin-treated Fli-1$^{+/-}$ mice than in bleomycin-treated wild-type (WT) mice. Bleomycin injection for 4 weeks induced greater dermal thickness in Fli-1$^{+/-}$ mice than in WT mice (2.4 fold versus 1.8 fold; $P < 0.05$), while dermal thickness was comparable between PBS-treated Fli-1$^{+/-}$ mice and PBS-treated WT mice (Figure 1A). Masson's trichrome staining confirmed an increase in signal intensity in response to bleomycin treatment in both WT and Fli-1$^{+/-}$ mice, but more importantly, a slight-to-moderate increase in the signal intensity was detected

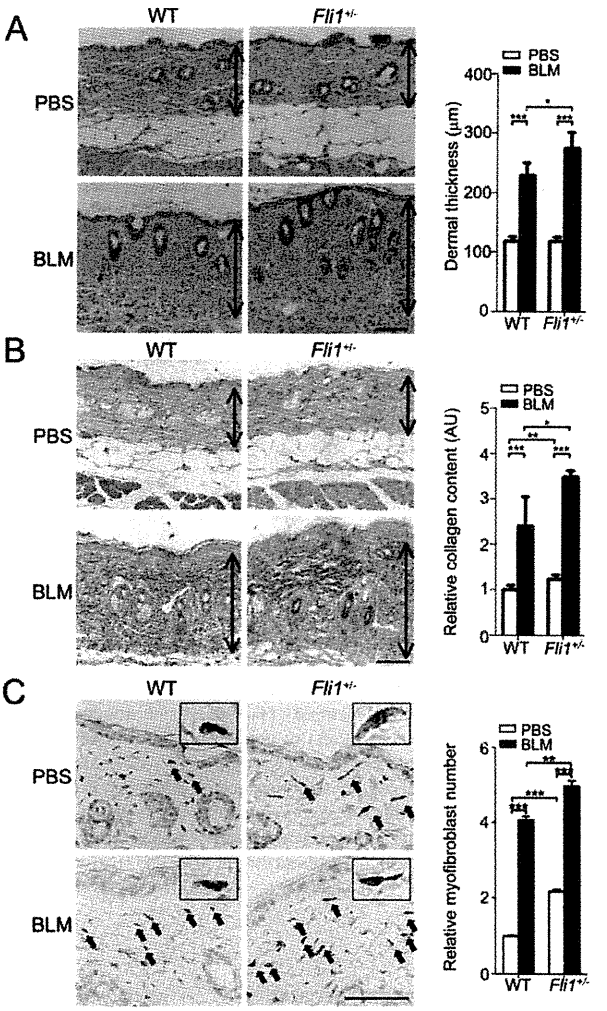

Figure 1. Exacerbation of bleomycin (BLM)–induced dermal fibrosis by Fli-1 haploinsufficiency. **A,** Left, Hematoxylin and eosin staining of representative skin sections from wild-type (WT) and Fli-1$^{+/-}$ mice on day 28 after phosphate buffered saline (PBS) or bleomycin injection. Bars = 50 μm. Right, Dermal thickness. **B,** Left, Masson's trichrome staining of representative skin sections from WT and Fli-1$^{+/-}$ mice on day 28 after PBS or bleomycin injection. Bars = 50 μm. Right, Collagen content, as measured by hydroxyproline assay. In **A** and **B,** values are the mean ± SEM (n = 4–8 mice per group). The relative ratio for each group is shown with the values for PBS-treated WT mice set at 1. **Arrows** indicate dermal thickness. **C,** Left, Representative skin histologic sections from WT and Fli-1$^{+/-}$ mice treated with PBS or bleomycin. Bars = 50 μm. **Insets** show higher-magnification views of fibroblasts. Right, Relative number of myofibroblasts in the dermis. The number per high-power field is adjusted to that in PBS-treated WT mice, which is set at 1. Values are the mean ± SEM (n = 4–5 mice per group). * = $P < 0.05$; ** = $P < 0.01$; *** = $P < 0.001$.

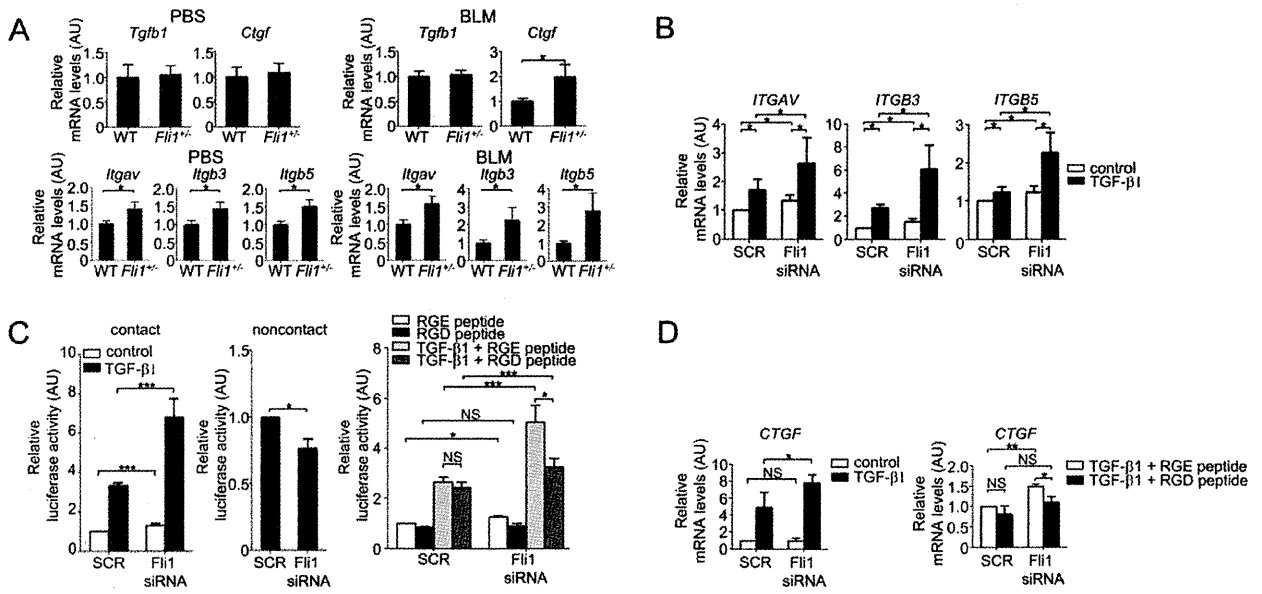

Figure 2. Amplification of bleomycin-induced expression of connective tissue growth factor (CTGF), $\alpha V\beta 3$ integrin, and $\alpha V\beta 5$ integrin in Fli-1–haploinsufficient dermal fibroblasts. **A,** Expression of mRNA for the *Tgfb1*, *Ctgf*, *Itgav*, *Itgb3*, and *Itgb5* genes in the mouse skin tissue on day 28 after PBS or bleomycin injection (n = 10 mice per group). **B,** Expression of mRNA for the *ITGAV*, *ITGB3*, and *ITGB5* genes in scrambled nonsilencing RNA (SCR)–treated or Fli-1 small interfering RNA (siRNA)–transfected normal human dermal fibroblasts left untreated or treated with transforming growth factor $\beta 1$ (TGFβ1; n = 6 samples per group). **C,** Luciferase activity in transformed mink lung reporter cells (TMLCs) cocultured in the presence (left) or absence (middle) of cell–cell contact with scrambled nonsilencing RNA– or Fli-1 siRNA–transfected dermal fibroblasts left untreated or treated with TGFβ1 (n= 4–6 samples per group), and luciferase activity in TMLCs cocultured in the presence of RGD or RGE peptides with scrambled nonsilencing RNA– or Fli-1 siRNA–transfected dermal fibroblasts left untreated or treated with TGFβ1 (n = 6 samples per group) (right). **D,** Expression of mRNA for the *CTGF* gene in scrambled nonsilencing RNA– or Fli-1 siRNA–transfected normal human dermal fibroblasts left untreated or treated with TGFβ1 (n = 4 samples per group) (left) and in scrambled nonsilencing RNA– or Fli-1 siRNA–transfected dermal fibroblasts treated with TGFβ1 in the presence of RGD or RGE peptides (n = 3 samples per group) (right). Values are the mean ± SEM. * = $P < 0.05$; ** = $P < 0.01$; *** = $P < 0.001$. NS = not significant (see Figure 1 for other definitions).

not only in bleomycin-treated Fli-$1^{+/-}$ mice compared with bleomycin-treated WT mice, but also in PBS-treated Fli-$1^{+/-}$ mice compared with PBS-treated WT mice (Figure 1B). This observation was confirmed by hydroxyproline assay (Figure 1B). Furthermore, the number of α-smooth muscle actin–positive cells showed the same trend, i.e., a significant elevation in both WT and Fli-$1^{+/-}$ mice in response to bleomycin treatment and in Fli-$1^{+/-}$ mice compared with WT mice after 4 weeks of PBS or bleomycin treatment (Figure 1C).

Thus, Fli-1 haploinsufficiency is sufficient to activate dermal fibroblasts in vivo and cooperatively establish tissue fibrosis together with additional factors induced by bleomycin. To elucidate the mechanism underlying this observation, we further investigated the impact of Fli-1 haploinsufficiency on fibroblasts, endothelial cells, and immune cells in vivo and in vitro. Since inflammation and dermal fibrosis peak on day 7 and day 28 after bleomycin injection, respectively (18,25–27), mouse skin samples obtained on day 7 and day 28 were used in the subsequent experiments.

Fli-1 haploinsufficiency cooperates with bleomycin to activate latent TGFβ through an $\alpha V\beta 3$ integrin– and $\alpha V\beta 5$ integrin–dependent mechanism, leading to CTGF induction. To assess the impact of Fli-1 haploinsufficiency on dermal fibroblasts, we first focused on TGFβ1 and CTGF. Fli-1 haploinsufficiency significantly increased *Ctgf* mRNA levels while not affecting *Tgfb1* mRNA levels in murine skin after 4 weeks of bleomycin injection (Figure 2A). Furthermore, CTGF was mainly expressed in the dermal fibroblasts of bleomycin-treated mice, as confirmed by colocalization of CTGF with FSP-1, a marker of fibroblasts, in double immunofluorescence (results are available online at http://www.h.u-tokyo.ac.jp/der/pg237.html). Given that TGFβ strongly induces CTGF expression in dermal fibroblasts and that CTGF is indispensable for the TGFβ-dependent induction and maintenance of dermal fibrosis in vivo (28), we

speculated that bleomycin may increase the sensitivity of Fli-1$^{+/-}$ mouse fibroblasts to TGFβ.

Since αVβ3 and αVβ5 integrins, receptors for the latent form of TGFβ, increase the sensitivity of SSc dermal fibroblasts to TGFβ by recruiting and activating latent TGFβ on the cell surface (22,29–31), the impact of Fli-1 deficiency on the expression of these integrins was investigated in vivo and in vitro. Levels of mRNA for *Itgav*, *Itgb3*, and *Itgb5* were modestly, but significantly increased at baseline in Fli-1$^{+/-}$ mice compared with WT mice, and bleomycin further potentiated expression of those genes, especially *Itgb3* and *Itgb5*, in Fli-1$^{+/-}$ mice, while a smaller increase was observed in WT mice (Figure 2A). Immunostaining confirmed the elevated expression of these integrins, especially in dermal fibroblasts, at the protein level (results are available online at http://www.h.u-tokyo.ac.jp/der/pg237.html). Consistent with these findings, Fli-1 siRNA, which achieved an ~73% reduction in Fli-1 mRNA levels, significantly but moderately increased the levels of mRNA for *ITGAV*, *ITGB3*, and *ITGB5* compared with scrambled nonsilencing RNA in normal human dermal fibroblasts (1.3, 1.6, and 1.3-fold increase, respectively; $P < 0.05$). Furthermore, TGFβ1 induced the expression of mRNA for *ITGB3* and *ITGB5* to a greater extent in Fli-1 siRNA–treated fibroblasts compared with scrambled nonsilencing RNA–treated fibroblasts (2.3-fold and 1.9-fold increase, respectively; $P < 0.05$). In contrast, TGFβ1 did not change the fold increase in mRNA expression for *ITGAV* triggered by Fli-1 siRNA treatment (1.5-fold increase; $P = 0.34$), although there was a significant difference in mRNA expression for *ITGAV* between Fli-1 siRNA– and scrambled nonsilencing RNA–transfected dermal fibroblasts treated with TGFβ1 (Figure 2B).

To gain further insights into the Fli-1–dependent activation of latent TGFβ, we used a TGFβ bioassay. Fli-1 siRNA–treated or scrambled nonsilencing RNA–treated normal human dermal fibroblasts were cultured with TMLCs, a mink lung epithelial reporter cell line stably expressing a portion of the plasminogen activator inhibitor 1 promoter (32). When cultured as a mixture with fibroblasts, luciferase activity was significantly higher in TMLCs cocultured with Fli-1 siRNA–treated fibroblasts than in those cocultured with scrambled nonsilencing RNA–treated fibroblasts (1.20-fold increase; $P < 0.01$) (Figure 2C). In contrast, when coculture assays were conducted with inserts to separate TMLCs and fibroblasts while allowing soluble molecules to pass, TMLCs cocultured with Fli-1 siRNA–treated fibroblasts showed significantly lower induction of luciferase activity than those cocultured with scrambled nonsilencing RNA–treated fibroblasts (0.78-fold decrease; $P < 0.05$) (Figure 2C).

These results, which are consistent with the findings of previous studies (22,30), indicate that a decrease in soluble activated TGFβ in the cultured medium of Fli-1 siRNA–treated fibroblasts is likely due to the activation of endogenous latent TGFβ and subsequent consumption by fibroblasts. Given that Fli-1 siRNA–dependent induction of luciferase activity was quite weak despite the high sensitivity of the TGFβ bioassay, the modest increase in αVβ3 and αVβ5 expression by Fli-1 haploinsufficiency is likely to be insufficient for the induction of TGFβ-dependent genes, including CTGF.

Since exogenous active TGFβ1 greatly increases these integrins in Fli-1 siRNA–treated fibroblasts, a TGFβ bioassay was also performed with Fli-1 siRNA–treated or scrambled nonsilencing RNA–treated fibroblasts stimulated with active TGFβ1 before coculture. Notably, pretreatment with active TGFβ1 further enhanced luciferase activity in TMLCs cocultured with Fli-1 siRNA–treated fibroblasts compared with those cocultured with scrambled nonsilencing RNA–treated fibroblasts (2.04-fold increase; $P < 0.01$) (Figure 2C). Furthermore, an RGD peptide that blocks the binding of αVβ3 and αVβ5 to latent TGFβ abolished elevated luciferase activity completely in TMLCs cocultured with Fli-1 siRNA–treated fibroblasts and also greatly reduced this activity in TMLCs cocultured with Fli-1 siRNA–treated fibroblasts prestimulated with active TGFβ1. In contrast, RGD treatment had a negligible effect on scrambled nonsilencing RNA–transfected fibroblasts pretreated with active TGFβ1 (Figure 2C), suggesting that the combination of Fli-1 siRNA and exogenous TGFβ1 activates latent TGFβ in part through an integrin-mediated mechanism.

To elucidate the impact of integrin-dependent latent TGFβ activation on CTGF expression, we further evaluated *CTGF* mRNA levels in Fli-1 siRNA–treated or scrambled nonsilencing RNA–treated normal human dermal fibroblasts stimulated with TGFβ1. TGFβ1 induced the expression of the *CTGF* gene to a greater extent in Fli-1 siRNA–treated fibroblasts than in scrambled nonsilencing RNA–treated fibroblasts, while *CTGF* mRNA levels were comparable without TGFβ1 treatment (Figure 2D). Furthermore, RGD peptide suppressed the expression of the *CTGF* gene in Fli-1 siRNA–treated fibroblasts stimulated with TGFβ1 to the levels comparable with those in scrambled nonsilencing RNA–treated fibroblasts stimulated with TGFβ1 (Figure 2D). These results indicate that gene silencing of Fli-1 augments exogenous TGFβ-dependent CTGF induction through αVβ3 integrin– and αVβ5 integrin–

dependent activation of latent TGFβ in dermal fibroblasts. Overall, these experiments strongly suggest that bleomycin in cooperation with Fli-1 haploinsufficiency induces fibrogenic genes, including CTGF, at least partly through the integrin-mediated activation of latent TGFβ.

Enhancement of endothelial-to-mesenchymal transition in response to bleomycin by Fli-1 haploinsufficiency. Endothelial-to-mesenchymal transition is a mechanism underlying pathologic fibrosis, including bleomycin-induced pulmonary fibrosis (33–36). Therefore, we investigated whether Fli-1 haploinsufficiency facilitates bleomycin-induced endothelial-to-mesenchymal transition by double immunofluorescence for FSP-1 and VE-cadherin (Figures 3A and B). Bleomycin-treated Fli-$1^{+/-}$ mice showed a greater number of FSP-1/VE-cadherin double-positive cells distributed in the lower dermis than bleomycin-treated WT mice. Notably, FSP-1/VE-cadherin double-positive cells were detected in the dermis of PBS-treated Fli-$1^{+/-}$ mice while absent in PBS-treated WT mice. In HDMECs, Fli-1 siRNA decreased the expression of mRNA for the endothelial marker VE-cadherin and increased the expression of mRNA for the mesenchymal markers *FSP1* and *ACTA2* and for *SNAI1*, an essential transcription factor regulating endothelial-to-mesenchymal transition (Figure 3C). Furthermore, Fli-1 occupied the promoter regions of the *FSP1* and *SNAI1* genes (Figure 3D) in addition to the previously reported VE-cadherin gene (16). Thus, Fli-1 deficiency directly contributes to endothelial-to-mesenchymal transition, and this process is further facilitated by bleomycin-induced factors.

Fli-1 haploinsufficiency modulates the expression of cell adhesion molecules related to a skewed T helper cell response. We previously demonstrated that the increased infiltration of mast cells and macrophages and the preferential polarization toward Th2 and Th17 phenotypes contribute to the development of bleomycin-induced dermal fibrosis in mice (37). Furthermore, we demonstrated that Th2/Th17 polarization depends on the expression of intercellular adhesion molecule 1 (ICAM-1) and glycosylation-dependent cell adhesion molecule 1 (GlyCAM-1) acting as positive regulators and P-selectin and E-selectin as negative regulators of these processes (37). Therefore, we next investigated the impact of Fli-1 on cell adhesion molecules in vivo and in vitro. The levels of mRNA for the *Icam1* and *Glycam1* genes were increased, while those of the *Selp* and *Sele* genes were decreased in bleomycin-treated Fli-$1^{+/-}$ mice compared with bleomycin-treated WT mice on day 7 (Figure 4A). Furthermore, Fli-1 siRNA, which achieved an 89% reduction in *Fli1* mRNA levels,

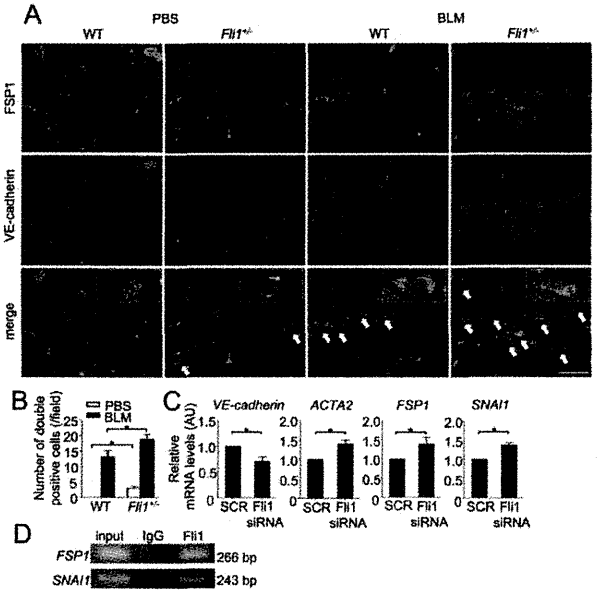

Figure 3. Endothelial-to-mesenchymal transition is directly induced by Fli-1 haploinsufficiency and further facilitated by bleomycin (BLM). **A,** Immunofluorescence staining for FSP-1 (green) and VE-cadherin (red) in skin samples from wild-type (WT) mice and Fli-$1^{+/-}$ mice treated with phosphate buffered saline (PBS) or bleomycin. **Arrows** indicate FSP-1/VE-cadherin double-positive cells. **Insets** show a higher-magnification view of representative cells (an FSP-1 single-positive cell for PBS-treated WT mice and double-positive cells for bleomycin-treated WT mice and PBS- and bleomycin-treated Fli-$1^{+/-}$ mice). Bar = 20 μm. **B,** Number of FSP-1/VE-cadherin double-positive cells per field (counted under magnification × 200). **C,** Expression of mRNA for the *VE-cadherin*, *ACTA2*, *FSP1*, and *SNAI1* genes in human dermal microvascular endothelial cells transfected with scrambled nonsilencing RNA or Fli-1 siRNA. In **B** and **C,** values are the mean ± SEM (n = 4 mice per group in **B** and 6 samples per group in **C**). * = $P < 0.05$. **D,** Chromatin immunoprecipitation analysis of Fli-1 binding to the promoters of the *FSP1* and *SNAI1* genes. See Figure 2 for other definitions. Color figure can be viewed in the online issue, which is available at http://onlinelibrary.wiley.com/doi/10.1002/art.38948/abstract.

significantly increased the levels of mRNA for the *ICAM1* and *GlyCAM1* genes while decreasing those of the *SELP* and *SELE* genes in HDMECs (Figure 4B). Moreover, Fli-1 occupied the promoter regions of the *ICAM1*, *SELP*, and *SELE* genes (Figure 4C). Taken together, these results indicate that Fli-1 haploinsufficiency directly modulates the expression of cell adhesion molecules, leading to the promotion of profibrotic inflammatory cell infiltration and Th2/Th17-dominant immune polarization in bleomycin-treated mice.

Reproduction of the expression profiles of cytokines and chemokines characteristic of SSc by Fli-1 haploinsufficiency. We next examined the levels of mRNA for various cytokines and chemokines implicated

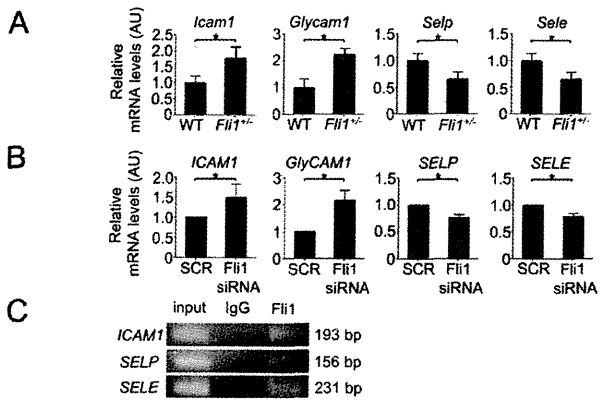

Figure 4. Fli-1 haploinsufficiency modulates the expression of cell adhesion molecules in dermal microvascular endothelial cells, leading to the induction of Th2/Th17-skewed inflammation. **A,** Levels of mRNA for the *Icam1*, *Glycam1*, *Selp*, and *Sele* genes in the skin of wild-type (WT) and Fli-1$^{+/-}$ mice treated with bleomycin for 7 days. **B,** Levels of mRNA for the *ICAM1*, *GlyCAM1*, *SELP*, and *SELE* genes in human dermal microvascular endothelial cells transfected with scrambled nonsilencing RNA (SCR) or Fli-1 small interfering RNA (siRNA). Values in **A** and **B** are the mean ± SEM (n = 10 mice per group in **A** and 6 samples per group in **B**). * = $P < 0.05$. **C,** Chromatin immunoprecipitation analysis of Fli-1 binding to the promoters of the *ICAM1*, *SELP*, and *SELE* genes.

in the pathogenesis of SSc in the lesional skin of mice. The levels of mRNA for *Il1b*, *Il4*, *Il6*, *Il10*, *Il17a*, *Ifng*, *Tnfa*, and *Mcp1* were significantly higher, and those of *Il12a* were significantly lower, in bleomycin-treated Fli-1$^{+/-}$ mice than in bleomycin-treated WT mice on day 7 (Figure 5A), while the levels were comparable between PBS-treated Fli-1$^{+/-}$ and WT mice (results are available online at http://www.h.u-tokyo.ac.jp/der/pg237.html). Thus, Fli-1 haploinsufficiency augments the expression levels of cytokines and chemokines characteristic of SSc in the lesional skin of bleomycin-treated mice.

Increased numbers of macrophages and mast cells and ratio of CD4+ to CD8+ T cells in the lesional skin of bleomycin-treated Fli-1$^{+/-}$ mice. We next evaluated the phenotype of immune cells in the lesional skin of bleomycin-treated Fli-1$^{+/-}$ mice. The number of macrophages and mast cells was markedly increased in bleomycin-treated Fli-1$^{+/-}$ mice compared with bleomycin-treated WT mice on day 7 and day 28 (Figure 5B) (additional results are available online at http://www.h.u-tokyo.ac.jp/der/pg237.html). In contrast, the number of CD4+ and CD8+ cells was decreased on day 7 and day 28, while the CD4+:CD8+ ratio was significantly increased on day 7, in bleomycin-treated Fli-1$^{+/-}$ mice compared with bleomycin-treated WT mice (Figure 5C) (additional results are available online at http://www.h.u-tokyo.ac.jp/der/pg237.html). Given that the numbers of macrophages, especially alternatively activated macrophages (M2 macrophages), and mast cells and the ratio of CD4+:CD8+ T cells are increased in the lesional skin of early diffuse cutaneous SSc (38,39), these data suggest that Fli-1 haploinsufficiency supports the development of an SSc-like immune response in the lesional skin of bleomycin-treated mice.

Fli-1 haploinsufficiency promotes M2 macrophage infiltration in the lesional skin of bleomycin-treated mice and M2 differentiation of peritoneal macrophages upon stimulation with IL-4 or IL-13. Since M2 differentiation of macrophages promotes tissue fibrosis

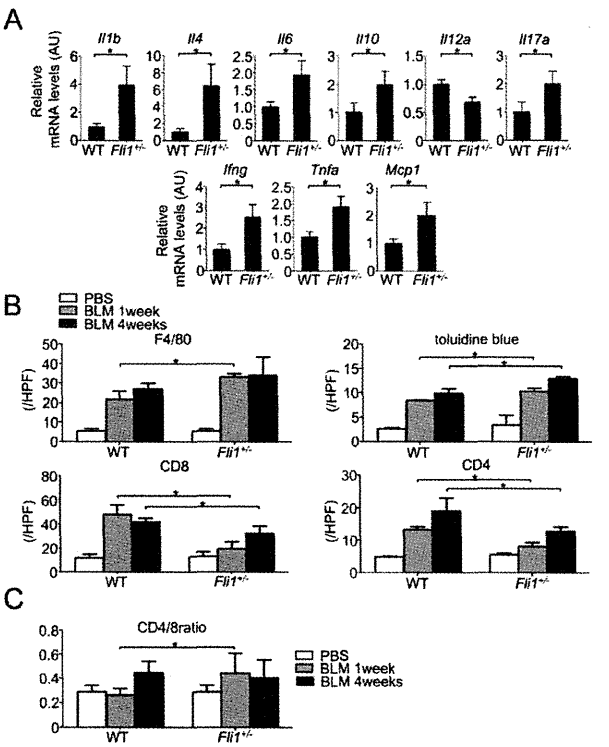

Figure 5. Fli-1 haploinsufficiency induces the expression profiles of cytokines and chemokines characteristic of systemic sclerosis (SSc) and promotes an SSc-like inflammatory infiltration in bleomycin-treated mice. **A,** Levels of mRNA for the *Il1b*, *Il4*, *Il6*, *Il10*, *Il12a*, *Il17a*, *Ifng*, *Tnfa*, and *Mcp1* genes in the skin of WT and Fli-1$^{+/-}$ mice on day 7 after bleomycin injection (n = 10 mice per group). **B,** Number of macrophages, mast cells, CD8+ T cells, and CD4+ T cells in the lesional skin of PBS- and bleomycin-treated WT mice and Fli-1$^{+/-}$ mice on days 7 and 28 (n = 5 mice per group). **C,** Ratio of CD4+ to CD8+ T cells in the lesional skin of PBS-treated and bleomycin-treated WT mice and Fli-1$^{+/-}$ mice on days 7 and 28 (n = 5 mice per group). Cells were counted in 10 random grids in 400× high-power fields (hpf). Values are the mean ± SEM. * = $P < 0.05$. See Figure 1 for other definitions.

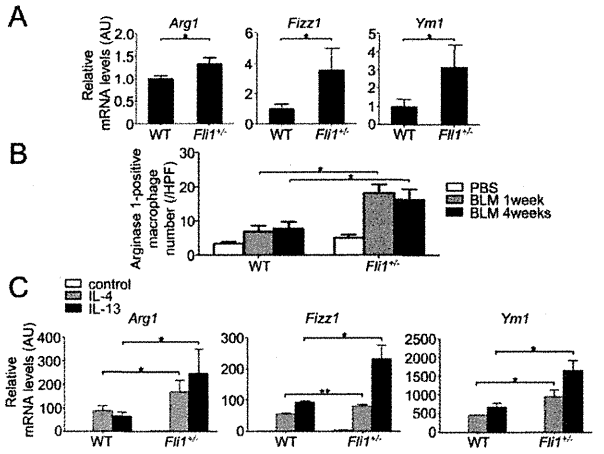

Figure 6. Fli-1 haploinsufficiency promotes M2 macrophage infiltration in the skin of bleomycin-treated mice and M2 differentiation of peritoneal macrophages upon interleukin-4 (IL-4) or IL-13 stimulation. **A,** Levels of mRNA for the *Arg1*, *Fizz1*, and *Ym1* genes in the skin of WT and Fli-1$^{+/-}$ mice on day 7 after bleomycin injection (n = 10 mice per group). **B,** Number of arginase 1–positive macrophages in the skin of WT and Fli-1$^{+/-}$ mice on day 7 and day 28 after injection with PBS or bleomycin (n = 5 mice per group). **C,** Levels of mRNA for the *Arg1*, *Fizz1*, and *Ym1* genes in peritoneal macrophages from WT and Fli-1$^{+/-}$ mice treated with IL-4 or IL-13 (n = 4 mice per group). Values are the mean ± SEM. * = $P < 0.05$; ** = $P < 0.01$. hpf = high-power field (see Figure 1 for other definitions).

in various pathologic conditions (40–42), including SSc (39,43,44), we next investigated if Fli-1 haploinsufficiency promotes M2 differentiation of macrophages. Levels of mRNA for the M2 macrophage markers *Arg1*, *Fizz1*, and *Ym1* were significantly elevated in Fli-1$^{+/-}$ mice compared with WT mice on day 7 (Figure 6A), while comparable at baseline (results are available online at http://www.h.u-tokyo.ac.jp/der/pg237.html). Consistent with these findings, the number of arginase 1–positive macrophages in the lesional skin was significantly increased in Fli-1$^{+/-}$ mice compared with WT mice on day 7 (Figure 6B). In addition, IL-4 and IL-13 induced polarization of macrophages toward the M2 phenotype to a greater extent in peritoneal macrophages isolated from Fli-1+/− mice than in those from WT mice (Figure 6C). Collectively, these results indicate that Fli-1 haploinsufficiency promotes M2 macrophage infiltration in the lesional skin of bleomycin-treated mice by inducing M2 differentiation of macrophages via an intrinsic mechanism triggered by bleomycin.

DISCUSSION

In this study, we demonstrated that Fli-1 haploinsufficiency exacerbates bleomycin-induced dermal fibrosis through multiple mechanisms, including induction of an SSc-like phenotype in dermal fibroblasts, endothelial cells, and macrophages; Th2/Th17-polarized inflammation; and increased mast cell infiltration. These results support the concept of the multifactorial nature of SSc and indicate that Fli-1 deficiency is a predisposing factor for this disease.

Fli-1 is a potent repressor of the *COL1A1* and *COL1A2* genes, and its down-regulation is a critical step in inducing matrix gene expression in dermal fibroblasts (4,6–10). In the skin of Fli-1$^{+/-}$ mice, mRNA levels for the *Col1a2* gene were markedly increased, and the levels of soluble type I collagen were also elevated (results are available online at http://www.h.u-tokyo.ac.jp/der/pg237.html), indicating that Fli-1 haploinsufficiency activates dermal fibroblasts in vivo. However, dermal thickness was comparable between Fli-1$^{-/-}$ and WT mice. While counterintuitive, this observation is plausible because there was no difference between Fli-1$^{+/-}$ and WT mice in CTGF expression, which is indispensable to establish and maintain dermal fibrosis in vivo (28,45,46). Supporting this notion, bleomycin increased CTGF expression as well as dermal thickness to a greater extent in Fli-1$^{+/-}$ mice than in WT mice. Although the detailed mechanism underlying the bleomycin-dependent CTGF induction in Fli-1$^{+/-}$ mouse dermal fibroblasts has not been fully elucidated, up-regulated expression of $\alpha V\beta 3$ and $\alpha V\beta 5$ integrins and activation of latent TGFβ may contribute to the enhanced expression of profibrotic genes, including CTGF. Indeed, it was recently reported that the αV-containing integrins collectively regulate the key profibrotic pathways during organ fibrosis (47).

Aberrant vascular activation plays a central role, together with inflammation and autoimmunity, in the initiation and maintenance of tissue fibrosis in SSc. Since endothelial cell–specific Fli-1–knockout mice reproduce the histologic abnormalities and increased vascular permeability characteristic of SSc, Fli-1 deficiency is also a potential predisposing factor for SSc vascular activation. To explore if Fli-1 deficiency links vascular events to tissue fibrosis in SSc, we evaluated the impact of Fli-1 haploinsufficiency on cell adhesion molecules regulating Th2/Th17-skewed inflammation and on endothelial-to-mesenchymal transition. Levels of the profibrotic cell adhesion molecules ICAM-1 and GlyCAM-1 were increased, while the antifibrotic cell adhesion molecules P-selectin and E-selectin were decreased in bleomycin-treated Fli-1$^{+/-}$ mice, which theoretically promotes Th2/Th17-skewed immune polarization. Consistent with these findings, the expression levels of the *Il4*, *Il6*, *Il10*, and *Il17a* genes were elevated, while those of the *Il12a*

gene were decreased in bleomycin-treated Fli-1$^{+/-}$ mice on day 7.

Given that immune polarization in diffuse cutaneous SSc generally shifts from Th2/Th17 to Th1 in parallel with disease duration and that levels of mRNA for the *ICAM1* and *GlyCAM1* genes are relatively higher than those of the *SELP* and *SELE* genes in the skin of early diffuse cutaneous SSc (results are available online at http://www.h.u-tokyo.ac.jp/der/pg237.html), the altered expression of cell adhesion molecules in endothelial cells due to Fli-1 deficiency may contribute to the induction of inflammatory cell infiltration characteristic of SSc. Furthermore, in contrast to PBS-treated WT mice, endothelial-to-mesenchymal transition was observed in PBS-treated Fli-1$^{+/-}$ mice and was induced to a greater extent in bleomycin-treated Fli-1$^{+/-}$ mice than in bleomycin-treated WT mice. Importantly, key molecules regulating endothelial-to-mesenchymal transition, including VE-cadherin, FSP-1, and Snai-1, were shown to be the direct targets of Fli-1. Taken together, these findings indicate that Fli-1 deficiency potentially promotes the induction of a profibrotic phenotype in dermal microvascular endothelial cells, especially in the presence of certain environmental influences in SSc.

The monocyte/macrophage lineages are characterized by considerable diversity and plasticity, which is regulated by a complicated network of signaling molecules, transcription factors, and epigenetic mechanisms. The present study demonstrates that Fli-1 haploinsufficiency promotes the expansion of M2 macrophages in the lesional skin of bleomycin-treated mice and M2 differentiation of peritoneal macrophages in response to IL-4 or IL-13 stimulation in vitro, suggesting that Fli-1 haploinsufficiency could directly contribute to the differentiation of M2 macrophages. Given that M2 macrophages represent the predominant macrophage subset in the lesional skin of early diffuse cutaneous SSc (39), Fli-1 haploinsufficiency may also serve as a predisposing factor to induce the SSc phenotype in response to environmental influences in macrophages.

Another important observation in this study was that Fli-1 haploinsufficiency increased mast cell infiltration and the CD4+:CD8+ ratio of infiltrating lymphocytes upon bleomycin treatment in the lesional skin. In SSc patients, it has been demonstrated that mast cells are increased and serve as a major producer of TGFβ in the lesional skin and that the CD4+:CD8+ ratio is increased in the peripheral blood and the lesional skin (38,48). Although the detailed mechanisms regulating mast cell infiltration and the significance of the elevated CD4+:CD8+ ratio are not well understood, the present finding further supports the idea that Fli-1 deficiency is also a predisposing factor integrating the induction of the SSc phenotype in various inflammatory cells.

In summary, this study provides strong evidence for the fundamental role of Fli-1 deficiency in inducing SSc-like phenotypic alterations in dermal fibroblasts, endothelial cells, and macrophages in a manner consistent with human disease. These results support the canonical idea that epigenetic reprogramming underlies pathogenic changes in SSc and implicate the Fli-1 deficiency–dependent pathway as a central mediator of this disease.

AUTHOR CONTRIBUTIONS

All authors were involved in drafting the article or revising it critically for important intellectual content, and all authors approved the final version to be published. Dr. Asano had full access to all of the data in the study and takes responsibility for the integrity of the data and the accuracy of the data analysis.

Study conception and design. Taniguchi, Asano, Trojanowska, Sato.
Acquisition of data. Taniguchi.
Analysis and interpretation of data. Taniguchi, Asano, Akamata, Noda, Takahashi, Ichimura, Toyama, Trojanowska, Sato.

REFERENCES

1. Asano Y. Future treatments in systemic sclerosis. J Dermatol 2010;37:54–70.
2. Asano Y, Sato S. Animal models of scleroderma: current state and recent development. Curr Rheumatol Rep 2013;15:382.
3. Wang Y, Fan PS, Kahaleh B. Association between enhanced type I collagen expression and epigenetic repression of the FLI1 gene in scleroderma fibroblasts. Arthritis Rheum 2006;54:2271–9.
4. Asano Y, Czuwara J, Trojanowska M. Transforming growth factor-β regulates DNA binding activity of transcription factor Fli1 by p300/CREB-binding protein-associated factor-dependent acetylation. J Biol Chem 2007;282:34672–83.
5. Chrobak I, Lenna S, Stawski L, Trojanowska M. Interferon-γ promotes vascular remodeling in human microvascular endothelial cells by upregulating endothelin (ET)-1 and transforming growth factor (TGF) β2. J Cell Physiol 2013;228:1774–83.
6. Asano Y, Trojanowska M. Phosphorylation of Fli1 at threonine 312 by protein kinase C δ promotes its interaction with p300/CREB-binding protein-associated factor and subsequent acetylation in response to transforming growth factor β. Mol Cell Biol 2009;29:1882–94.
7. Kubo M, Czuwara-Ladykowska J, Moussa O, Markiewicz M, Smith E, Silver RM, et al. Persistent down-regulation of Fli1, a suppressor of collagen transcription, in fibrotic scleroderma skin. Am J Pathol 2003;163:571–81.
8. Asano Y, Markiewicz M, Kubo M, Szalai G, Watson DK, Trojanowska M. Transcription factor Fli1 regulates collagen fibrillogenesis in mouse skin. Mol Cell Biol 2009;29:425–34.
9. Czuwara-Ladykowska J, Shirasaki F, Jackers P, Watson DK, Trojanowska M. Fli-1 inhibits collagen type I production in dermal fibroblasts via an Sp1-dependent pathway. J Biol Chem 2001;276:20839–48.
10. Nakerakanti SS, Kapanadze B, Yamasaki M, Markiewicz M, Trojanowska M. Fli1 and Ets1 have distinct roles in connective tissue growth factor/CCN2 gene regulation and induction of the profibrotic gene program. J Biol Chem 2006;281:25259–69.
11. Noda S, Asano Y, Akamata K, Aozasa N, Taniguchi T, Takahashi T, et al. A possible contribution of altered cathepsin B expression to the development of skin sclerosis and vasculopathy in systemic sclerosis. PLoS One 2012;7:e32272.

12. Noda S, Asano Y, Takahashi T, Akamata K, Aozasa N, Taniguchi T, et al. Decreased cathepsin V expression due to Fli1 deficiency contributes to the development of dermal fibrosis and proliferative vasculopathy in systemic sclerosis. Rheumatology (Oxford) 2013; 52:790–9.
13. Chan ES, Liu H, Fernandez P, Luna A, Perez-Aso M, Bujor AM, et al. Adenosine A_{2A} receptors promote collagen production by a Fli1- and CTGF-mediated mechanism. Arthritis Res Ther 2013; 15:R58.
14. Bujor AM, Haines P, Padilla C, Christmann RB, Junie M, Sampaio-Barros PD, et al. Ciprofloxacin has antifibrotic effects in scleroderma fibroblasts via downregulation of Dnmt1 and upregulation of Fli1. Int J Mol Med 2012;30:1473–80.
15. Nakerakanti SS, Bujor AM, Trojanowska M. CCN2 is required for the TGF-β induced activation of Smad1-Erk1/2 signaling network. PLoS One 2011;6:e21911.
16. Asano Y, Stawski L, Hant F, Highland K, Silver R, Szalai G, et al. Endothelial Fli1 deficiency impairs vascular homeostasis: a role in scleroderma vasculopathy. Am J Pathol 2010;176:1983–98.
17. Spyropoulos DD, Pharr PN, Lavenburg KR, Jackers P, Papas TS, Ogawa M, et al. Hemorrhage, impaired hematopoiesis, and lethality in mouse embryos carrying a targeted disruption of the Fli1 transcription factor. Mol Cell Biol 2000;20:5643–52.
18. Yamamoto T, Takagawa S, Katayama I, Yamazaki K, Hamazaki Y, Shinkai H, et al. Animal model of sclerotic skin. I. Local injections of bleomycin induce sclerotic skin mimicking scleroderma. J Invest Dermatol 1999;112:456–62.
19. Yoshizaki A, Iwata Y, Komura K, Ogawa F, Hara T, Muroi E, et al. CD19 regulates skin and lung fibrosis via Toll-like receptor signaling in a model of bleomycin-induced scleroderma. Am J Pathol 2008;172:1650–63.
20. Asano Y, Ihn H, Yamane K, Kubo M, Tamaki K. Impaired Smad7-Smurf-mediated negative regulation of TGF-β signaling in scleroderma fibroblasts. J Clin Invest 2004;113:253–64.
21. Zeini M, Traves PG, Lopez-Fontal R, Pantoja C, Matheu A, Serrano M, et al. Specific contribution of p19(ARF) to nitric oxide-dependent apoptosis. J Immunol 2006;177:3327–36.
22. Asano Y, Ihn H, Yamane K, Jinnin M, Tamaki K. Increased expression of integrin $\alpha V\beta 5$ induces the myofibroblastic differentiation of dermal fibroblasts. Am J Pathol 2006;168:499–510.
23. Miller EJ, Rhodes RK. Preparation and characterization of the different types of collagen. Methods Enzymol 1982;82 Pt A:33–64.
24. Markiewicz M, Asano Y, Znoyko S, Gong Y, Watson DK, Trojanowska M. Distinct effects of gonadectomy in male and female mice on collagen fibrillogenesis in the skin. J Dermatol Sci 2007;47:217–26.
25. Yamamoto T, Takahashi Y, Takagawa S, Katayama I, Nishioka K. Animal model of sclerotic skin. II. Bleomycin induced scleroderma in genetically mast cell deficient WBB6F1-W/Wv mice. J Rheumatol 1999;26:2628–34.
26. Yamamoto T, Kuroda M, Nishioka K. Animal model of sclerotic skin. III. Histopathological comparison of bleomycin-induced scleroderma in various mice strains. Arch Dermatol Res 2000;292: 535–41.
27. Takagawa S, Lakos G, Mori Y, Yamamoto T, Nishioka K, Varga J. Sustained activation of fibroblast transforming growth factor-β/Smad signaling in a murine model of scleroderma. J Invest Dermatol 2003;121:41–50.
28. Mori T, Kawara S, Shinozaki M, Hayashi N, Kakinuma T, Igarashi A, et al. Role and interaction of connective tissue growth factor with transforming growth factor-β in persistent fibrosis: a mouse fibrosis model. J Cell Physiol 1999;181:153–9.
29. Asano Y, Ihn H, Yamane K, Kubo M, Tamaki K. Increased expression levels of integrin $\alpha V\beta 5$ on scleroderma fibroblasts. Am J Pathol 2004;164:1275–92.
30. Asano Y, Ihn H, Yamane K, Jinnin M, Mimura Y, Tamaki K. Increased expression of integrin $\alpha V\beta 3$ contributes to the establishment of autocrine TGF-β signaling in scleroderma fibroblasts. J Immunol 2005;175:7708–18.
31. Asano Y, Ihn H, Yamane K, Jinnin M, Mimura Y, Tamaki K. Involvement of $\alpha V\beta 5$ integrin–mediated activation of latent transforming growth factor $\beta 1$ in autocrine transforming growth factor β signaling in systemic sclerosis fibroblasts. Arthritis Rheum 2005;52:2897–905.
32. Abe M, Harpel JG, Metz CN, Nunes I, Loskutoff DJ, Rifkin DB. An assay for transforming growth factor-β using cells transfected with a plasminogen activator inhibitor-1 promoter-luciferase construct. Anal Biochem 1994;216:276–84.
33. Kizu A, Medici D, Kalluri R. Endothelial-mesenchymal transition as a novel mechanism for generating myofibroblasts during diabetic nephropathy. Am J Pathol 2009;175:1371–3.
34. Zeisberg EM, Tarnavski O, Zeisberg M, Dorfman AL, McMullen JR, Gustafsson E, et al. Endothelial-to-mesenchymal transition contributes to cardiac fibrosis. Nat Med 2007;13:952–61.
35. Li J, Qu X, Bertram JF. Endothelial-myofibroblast transition contributes to the early development of diabetic renal interstitial fibrosis in streptozotocin-induced diabetic mice. Am J Pathol 2009;175:1380–8.
36. Hashimoto N, Phan SH, Imaizumi K, Matsuo M, Nakashima H, Kawabe T, et al. Endothelial-mesenchymal transition in bleomycin-induced pulmonary fibrosis. Am J Respir Cell Mol Biol 2010;43: 161–72.
37. Yoshizaki A, Yanaba K, Iwata Y, Komura K, Ogawa A, Akiyama Y, et al. Cell adhesion molecules regulate fibrotic process via Th1/Th2/Th17 cell balance in a bleomycin-induced scleroderma model. J Immunol 2010;185:2502–15.
38. Hussein MR, Hassan HI, Hofny ER, Elkholy M, Fatehy NA, Abd Elmoniem AE, et al. Alterations of mononuclear inflammatory cells, CD4/CD8+ T cells, interleukin 1β, and tumour necrosis factor α in the bronchoalveolar lavage fluid, peripheral blood, and skin of patients with systemic sclerosis. J Clin Pathol 2005;58: 178–84.
39. Higashi-Kuwata N, Jinnin M, Makino T, Fukushima S, Inoue Y, Muchemwa FC, et al. Characterization of monocyte/macrophage subsets in the skin and peripheral blood derived from patients with systemic sclerosis. Arthritis Res Ther 2010;12:R128.
40. Ploeger DT, Hosper NA, Schipper M, Koerts JA, de Rond S, Bank RA. Cell plasticity in wound healing: paracrine factors of M1/M2 polarized macrophages influence the phenotypical state of dermal fibroblasts. Cell Commun Signal 2013;11:29.
41. Han Y, Ma FY, Tesch GH, Manthey CL, Nikolic-Paterson DJ. Role of macrophages in the fibrotic phase of rat crescentic glomerulonephritis. Am J Physiol Renal Physiol 2013;304: F1043–53.
42. Wang J, Jiang ZP, Su N, Fan JJ, Ruan YP, Peng WX, et al. The role of peritoneal alternatively activated macrophages in the process of peritoneal fibrosis related to peritoneal dialysis. Int J Mol Sci 2013;14:10369–82.
43. Hamilton RF, Parsley E, Holian A. Alveolar macrophages from systemic sclerosis patients: evidence for IL-4-mediated phenotype changes. Am J Physiol Lung Cell Mol Physiol 2004;286:L1202–9.
44. Mathai SK, Gulati M, Peng X, Russell TR, Shaw AC, Rubinowitz AN, et al. Circulating monocytes from systemic sclerosis patients with interstitial lung disease show an enhanced profibrotic phenotype. Lab Invest 2010;90:812–23.
45. Liu S, Shi-wen X, Abraham DJ, Leask A. CCN2 is required for bleomycin-induced skin fibrosis in mice. Arthritis Rheum 2011;63: 239–46.
46. Liu S, Parapuram SK, Leask A. Fibrosis caused by loss of PTEN expression in mouse fibroblasts is crucially dependent on CCN2. Arthritis Rheum 2013;65:2940–4.
47. Henderson NC, Arnold TD, Katamura Y, Giacomini MM, Rodriguez JD, McCarty JH, et al. Targeting of αV integrin identifies a core molecular pathway that regulates fibrosis in several organs. Nat Med 2013;19:1617–24.
48. Hugle T, Hogan V, White KE, van Laar JM. Mast cells are a source of transforming growth factor β in systemic sclerosis. Arthritis Rheum 2011;63:795–9.

ARTHRITIS & RHEUMATOLOGY
Vol. 67, No. 1, January 2015, pp 254–265
DOI 10.1002/art.38901

Amelioration of Tissue Fibrosis by Toll-like Receptor 4 Knockout in Murine Models of Systemic Sclerosis

Takehiro Takahashi, Yoshihide Asano, Yohei Ichimura, Tetsuo Toyama, Takashi Taniguchi, Shinji Noda, Kaname Akamata, Yayoi Tada, Makoto Sugaya, Takafumi Kadono, and Shinichi Sato

Objective. **Bleomycin-induced fibrosis and the tight skin (TSK/+) mouse are well-established experimental murine models of human systemic sclerosis (SSc). Growing evidence has demonstrated the pivotal role of Toll-like receptors (TLRs) in several autoimmune inflammatory diseases, including SSc. This study was undertaken to determine the role of TLR-4 in the fibrotic processes in these murine models.**

Methods. **We generated a murine model of bleomycin-induced SSc using TLR-4$^{-/-}$ mice and TLR-4$^{-/-}$;TSK/+ mice. The mechanisms by which TLR-4 contributes to pathologic tissue fibrosis were investigated in these 2 models by histologic examination, hydroxyproline assay, enzyme-linked immunosorbent assay, real-time polymerase chain reaction, and flow cytometry.**

Results. **Dermal and lung fibrosis was attenuated in bleomycin-treated TLR-4$^{-/-}$ mice compared with their wild-type counterparts. Inflammatory cell infiltration, expression of various inflammatory cytokines, and pathologic angiogenesis induced by bleomycin treatment were suppressed with TLR-4 deletion. Furthermore, the increased expression of interleukin-6 (IL-6) in fibroblasts, endothelial cells, and immune cells in response to bleomycin in vivo and to lipopolysaccharide in vitro was notably abrogated in the absence of TLR-4. Moreover, TLR-4 deletion was associated with alleviated B cell activation and skew toward a Th2/Th17 response against bleomycin treatment. Importantly, in TSK/+ mice, another SSc murine model, TLR-4 abrogation attenuated hypodermal fibrosis.**

Conclusion. **These results indicate the pivotal contribution of TLR-4 to the pathologic tissue fibrosis of SSc murine models. Our results indicate the critical role of TLR-4 signaling in the development of tissue fibrosis, suggesting that biomolecular TLR-4 targeting might be a potential therapeutic approach to SSc.**

Systemic sclerosis (SSc) is an autoimmune disorder characterized by initial vascular injuries and resultant fibrosis in the skin and certain internal organs (1). Numerous studies have shown that the complex interactions between leukocytes, endothelial cells, and fibroblasts lead to fibroblast activation and extracellular matrix overproduction (2). These interactions are mediated by several inflammatory cytokines, chemokines, growth factors, and adhesion molecules. Levels of interleukin-1 (IL-1), IL-4, IL-6, IL-13, IL-23, tumor necrosis factor α (TNFα), and monocyte chemotactic protein 1 (MCP-1) are elevated in the sera of SSc patients (3–6) and play critical roles in mouse models of bleomycin-induced SSc (7,8).

Imbalance between Th1 and Th2 cytokines throughout the disease course of SSc further suggests the primary roles of these factors (9). Th2 polarization is characteristic of early diffuse cutaneous SSc (dcSSc), while the balance shifts to Th1 predominance with the resolution of skin sclerosis, and persistent Th2 predominance is related to poor prognosis (10). Among these

Supported by the Ministry of Health, Welfare, and Labor of Japan (Health Science Research grants), the Ministry of Education, Culture, Sports, Science, and Technology of Japan, and the Japan Society for the Promotion of Science (Grant-in-Aid for JSPS Fellows no. 24-4204 to Dr. Takahashi).

Takehiro Takahashi, MD, Yoshihide Asano, MD, PhD, Yohei Ichimura, MD, Tetsuo Toyama, MD, Takashi Taniguchi, MD, Shinji Noda, MD, PhD, Kaname Akamata, MD, PhD, Yayoi Tada, MD, PhD, Makoto Sugaya, MD, PhD, Takafumi Kadono, MD, PhD, Shinichi Sato, MD, PhD: University of Tokyo Graduate School of Medicine, Tokyo, Japan.

Address correspondence to Yoshihide Asano, MD, PhD, or Shinichi Sato, MD, PhD, Department of Dermatology, University of Tokyo Graduate School of Medicine, 7-3-1 Hongo, Bunkyo-ku, Tokyo 113-8655, Japan. E-mail: yasano-tky@umin.ac.jp or satos-der@h.u-tokyo.ac.jp.

Submitted for publication November 21, 2013; accepted in revised form September 30, 2014.